

RESEARCH ARTICLE

Inhibition of microRNA suppression of *Dishevelled* results in Wnt pathway-associated developmental defects in sea urchin

Nina Faye Sampilo¹, Nadezda A. Stepicheva^{1,2}, Syed Aun Murtaza Zaidi¹, Lingyu Wang³, Wei Wu³, Athula Wikramanayake³ and Jia L. Song^{1,*}

ABSTRACT

MicroRNAs (miRNAs) are highly conserved, small non-coding RNAs that regulate gene expressions by binding to the 3' untranslated region of target mRNAs thereby silencing translation. Some miRNAs are key regulators of the Wnt signaling pathways, which impact developmental processes. This study investigates miRNA regulation of different isoforms of *Dishevelled* (*Dvl/Dsh*), which encode a key component in the Wnt signaling pathway. The sea urchin *Dvl* mRNA isoforms have similar spatial distribution in early development, but one isoform is distinctively expressed in the larval ciliary band. We demonstrated that *Dvl* isoforms are directly suppressed by miRNAs. By blocking miRNA suppression of *Dvl* isoforms, we observed dose-dependent defects in spicule length, patterning of the primary mesenchyme cells, gut morphology, and cilia. These defects likely result from increased Dvl protein levels, leading to perturbation of Wnt-dependent signaling pathways and additional Dvl-mediated processes. We further demonstrated that overexpression of *Dvl* isoforms recapitulated some of the *Dvl* miRNA-induced phenotypes. Overall, our results indicate that miRNA suppression of *Dvl* isoforms plays an important role in ensuring proper development and function of primary mesenchyme cells and cilia.

KEY WORDS: Sea urchin, Primary mesenchyme cells, miRNA target protector, Post-transcriptional regulation, Cilia

INTRODUCTION

Dishevelled is a key regulator in the highly conserved Wnt signaling pathway and plays the paramount role of directing signaling towards the different branches of Wnt signaling cascades (Gao and Chen, 2010). Components of the Wnt signaling pathways are expressed during early stages of embryonic development to specify cell fates, direct morphogenic movements, and maintain neuronal stem cells along with many other important functions (Gao and Chen, 2010; De, 2011). Upon Wnt ligand binding to the Frizzled (Fz) receptor, Dvl is recruited to the plasma membrane as it binds to Fz. Depending on which proteins interact with Dvl, it can activate either the canonical Wnt/ β -catenin (cWnt) signaling cascades important for cell specification, the non-canonical Wnt planar cell polarity (ncWnt/PCP) or the non-canonical Wnt calcium pathway (ncWnt/ Ca^{2+}) to control cellular morphogenesis (Gao and Chen, 2010; Song et al., 2015).

The cWnt signaling pathway is a highly conserved mechanism for germ layer specification in all metazoans (Moon, 2005; Komiya and Habas, 2008). Dvl has been shown to be required for animal-vegetal axial patterning, β -catenin stabilization, and endodermal specification in bilaterians, including echinoderms and chordates, and non-bilaterians such as the starlet sea anemone in the Cnidaria phylum (Lee et al., 2007; Kumburegama et al., 2011). Previously, it has been shown that both Dvl (Weitzel et al., 2004; Peng and Wikramanayake, 2013) and β -catenin (Logan et al., 1999) localize to the vegetal pole of the sea urchin embryo, resulting in activation of endodermal and mesodermal cell specification.

The ncWnt pathways are β -catenin independent and consist of the ncWnt/PCP and the ncWnt/ Ca^{2+} pathways. The ncWnt/PCP pathway regulates polarization of epithelial cells, enabling cell morphogenesis and tissue patterning. Mutation of ncWnt/PCP genes in vertebrates results in a broader and shorter body axis and neural tube closure defects due to blockage of cell movements (Simons and Mlodzik, 2008; Yin et al., 2009; Hayes et al., 2013). In *Drosophila*, PCP signaling is necessary for orientation of epithelial structures in the cuticle, wing and eye (Gubb and Garcia-Bellido, 1982; Adler, 2002; Sepich et al., 2011). The PCP pathway also consists of multiple genes required for ciliogenesis (Dale et al., 2009).

The ncWnt/ Ca^{2+} pathway, mediated by G-protein signaling, stimulates release of intracellular Ca^{2+} and activation of protein kinase C to control actin polymerization (Gao and Chen, 2010). In *Xenopus*, embryos were found to have elevated Ca^{2+} /CaMKII levels in the ventral side of the embryo (Kühl et al., 2000). In zebrafish, complete blockade of ncWnt/ Ca^{2+} leads to a variety of developmental defects, such as gut abnormalities and tumor formation (Yoshida et al., 2004; De, 2011).

The Dvl protein has three highly conserved domains: an N-terminal DIX (Dishevelled, Axin) domain, a central PDZ (Postsynaptic density 95, Discs Large, Zonula occludens-1) domain, and a C-terminal DEP (Dvl, Egl-10, Pleckstrin) domain (Gao and Chen, 2010). In general, the DIX domain of Dvl is important for Wnt/ β -catenin signaling, and the PDZ and DEP domains are both required for ncWnt/PCP and ncWnt/ Ca^{2+} pathways (Axelrod et al., 1998; Tada and Smith, 2000). In addition, Dvl-DEP and the C-terminal region (DEP-C) interact with three discontinuous regions of Fz. DEP-C binding to Fz stabilizes the binding of the Dvl-DEP domain to Fz, which is required to drive cWnt/ β -catenin activation in *Xenopus* and in HEK293T cells (Tauriello et al., 2012). Overexpression of Dvl-DIX in the sea urchin resulted in a lack of nuclear localization of β -catenin (Weitzel et al., 2004), in *Drosophila* resulted in a lack of β -catenin/Wnt activity (Axelrod et al., 1998), and in *Nematostella* resulted in a lack of archenteron and endodermal epithelium (Kumburegama et al., 2011). In *Xenopus*, overexpression of truncated Dvl possessing only PDZ and DEP domains relayed Wnt signaling predominantly via the ncWnt/ Ca^{2+} cascade, as seen

¹Department of Biological Sciences, University of Delaware, Newark, DE 19716, USA. ²Department of Ophthalmology, University of Pittsburgh School of Medicine, Pittsburgh, PA 15261, USA. ³Department of Biology, University of Miami, Coral Gables, FL 33124, USA.

*Author for correspondence (jsong@udel.edu)

DOI: 10.1242/dev.167130

in elevated levels of intracellular Ca^{2+} and activation of Ca^{2+} -dependent enzymes, such as PKC and Calcineurin (Komiya and Habas, 2008). Overexpression of Dvl-DEP in sea urchin, which blocks the ncWnt pathway through a dominant-negative mechanism, resulted in failed archenteron invagination (Byrum et al., 2009). Thus, depending on its interacting proteins, Dvl can direct various branches of the Wnt signaling pathways.

Relatively little is known of the impact of post-transcriptional regulation of Dvl on Wnt signaling pathways (He et al., 2015; Huang et al., 2018). MicroRNAs (miRNAs) are small non-coding RNAs that regulate post-transcriptional gene expression by binding to the 3' untranslated region (3'UTR) of target mRNAs to repress their translation and/or induce mRNA degradation (Bartel, 2009). Similar to vertebrates, each sea urchin miRNA has many predicted targets (Song et al., 2012; Stepicheva et al., 2015; Stepicheva and Song, 2015). Previous studies indicated that the sea urchin embryo contains approximately 50 miRNAs, of which *SpmiR-31* has been identified to target multiple genes important for primary mesenchyme cell (PMC) development and function (Song et al., 2012; Stepicheva and Song, 2015). Additionally, *SpmiRDeep2-30364*, and *SpmiR2007* have been shown to suppress β -catenin (Stepicheva et al., 2015). The overarching hypothesis of the current study is that miRNAs modulate components of the Wnt signaling pathways to provide crucial regulation that impacts cell functions and embryonic structures. Specifically, this study examines miRNA regulation of Dvl. We found that the sea urchin embryo harbors four isoforms of Dvl, three of which have unique 3'UTRs. We demonstrated that miRNAs directly suppress *Dvl5a* and *Dvl4a*. By removal of miRNA suppression of these Dvl isoforms, we observed dose-dependent defects in gut morphology, skeletal length and PMC patterning. In addition, we observed profound ciliary defects in the Dvl miRNATP-injected larvae that resulted in swimming defects. Importantly, overexpression of Dvl isoforms recapitulated the Dvl miRNATP-induced phenotypes. These results indicate that miRNAs modulate

the expression of Dvl isoforms thereby providing additional regulation to ensure proper embryonic development.

RESULTS

Sea urchin embryo has four Dishevelled isoforms

Four different isoforms of Dvl were identified from a previous RNA-Seq experiment in an effort to identify vegetal cortex-enriched mRNAs (L.W., W.W. and A.W., unpublished). All isoforms of *Strongylocentrotus purpuratus* Dvl (*SpDvl5a*, 1, 4a and 4b) share the exact same protein sequence except for the last exon. Only Dvl5a contains the highly conserved DEP-C domain (AMGNPSEFFVDVM) that is essential for interacting with Fz and its own Dvl-DEP domain to drive the cWnt/ β -catenin pathway (Fig. 1A) (Tauriello et al., 2012). Dvl from another sea urchin species, *Lytechinus variegatus*, *LvDvl*, and *SpDvl4a/4b* have C-terminal amino acid residues unique to the sea urchin species (YFDDSSVTLL) (Fig. 1A) (Weitzel et al., 2004). Dvl1 lacks the last exon and contains a unique three amino acid sequence (NPS) in the most C-terminal region. Despite close identity of their protein sequences, these *SpDvl* isoforms have three unique 3'UTRs (Fig. 1B). *Dvl4a* differs from *Dvl4b* only in their 3'UTRs, where miRNA regulation typically occurs (Selbach et al., 2008). *Dvl1* has the same 3'UTR as *Dvl4a*. Potential mRNA regulatory sites were bioinformatically identified by searching for inverse complementary miRNA seed sequences within the Dvl 3'UTRs (Song et al., 2012; Stepicheva et al., 2015; Stepicheva and Song, 2015). The precise regulation and function of each of these Dvl isoforms are not known.

Dishevelled isoforms are differentially expressed

We tested the expression of *Dvl5a*, *Dvl4a/1* and *Dvl4b* isoforms, using primers designed against their unique 3'UTRs. It was not possible to design *Dvl1*-specific primers owing to its high similarity with *Dvl4a* (Fig. S1). The expression of these Dvl



Fig. 1. Four isoforms of Dvl with shared protein domains and three unique 3'UTRs. (A) All *SpDvl* isoforms contain the conserved DIX, PDZ and DEP domains. Partial multiple alignment of Dvl C-terminus protein sequences from various species indicated that *SpDvl4a*, *SpDvl4b*, *SpDvl1* and *SpDvl5a* have different amino acids in the sequence encoded by the last exon. Only *SpDvl5a* contains the conserved DEP-C domain (highlighted in yellow). (B) The *SpDvl1* isoform lacks one exon at the end of its coding region and has an identical 3'UTR to *SpDvl4a*. *SpDvl5a*, *SpDvl4a/Dvl1* and *SpDvl4b* have unique 3'UTRs. The potential miRNA regulatory sites within *SpDvl* 3'UTRs were identified bioinformatically, based on the inverse complementary seed sequences that have a perfect match to the corresponding miRNA. Dvl miRNATPs used to block miRNA binding of the *SpDvl* transcripts are shown in blue. +1 is the first base pair of the 3'UTR.

isoforms were assayed at various developmental stages [0, 6, 24, 30 and 72 h post-fertilization (hpf)], using real-time, quantitative PCR (QPCR). We observed that all *Dvl* transcripts were expressed throughout development and increased steadily from the egg stage up until the gastrula stage. At the larval stage, the expression of all *Dvl* isoforms decreased (normalized to that of egg) (Fig. 2A).

To examine the temporal and spatial expression of *Dvl* isoforms in early development, we constructed RNA *in situ* probes complementary to distinct 3'UTRs from *Dvl5a*, *Dvl4a/Dvl1* and

Dvl4b isoforms. Note that the *in situ* probe against *Dvl4a* will also recognize *Dvl1* (Fig. S1). We observed that all *Dvl* isoforms were ubiquitously expressed during early stages of development. Interestingly, *Dvl4a/Dvl1* is enriched in the ciliary band of the larval stage (Fig. 2B).

We also examined the localization of Dvl protein at blastula, gastrula and plutei stages, using a pan-Dvl antibody (Peng and Wikramanayake, 2013). At the blastula and gastrula stages, Dvl was ubiquitously expressed and enriched in the posterior of the embryo. Dvl was also enriched in the gut and PMCs of gastrulae. At the

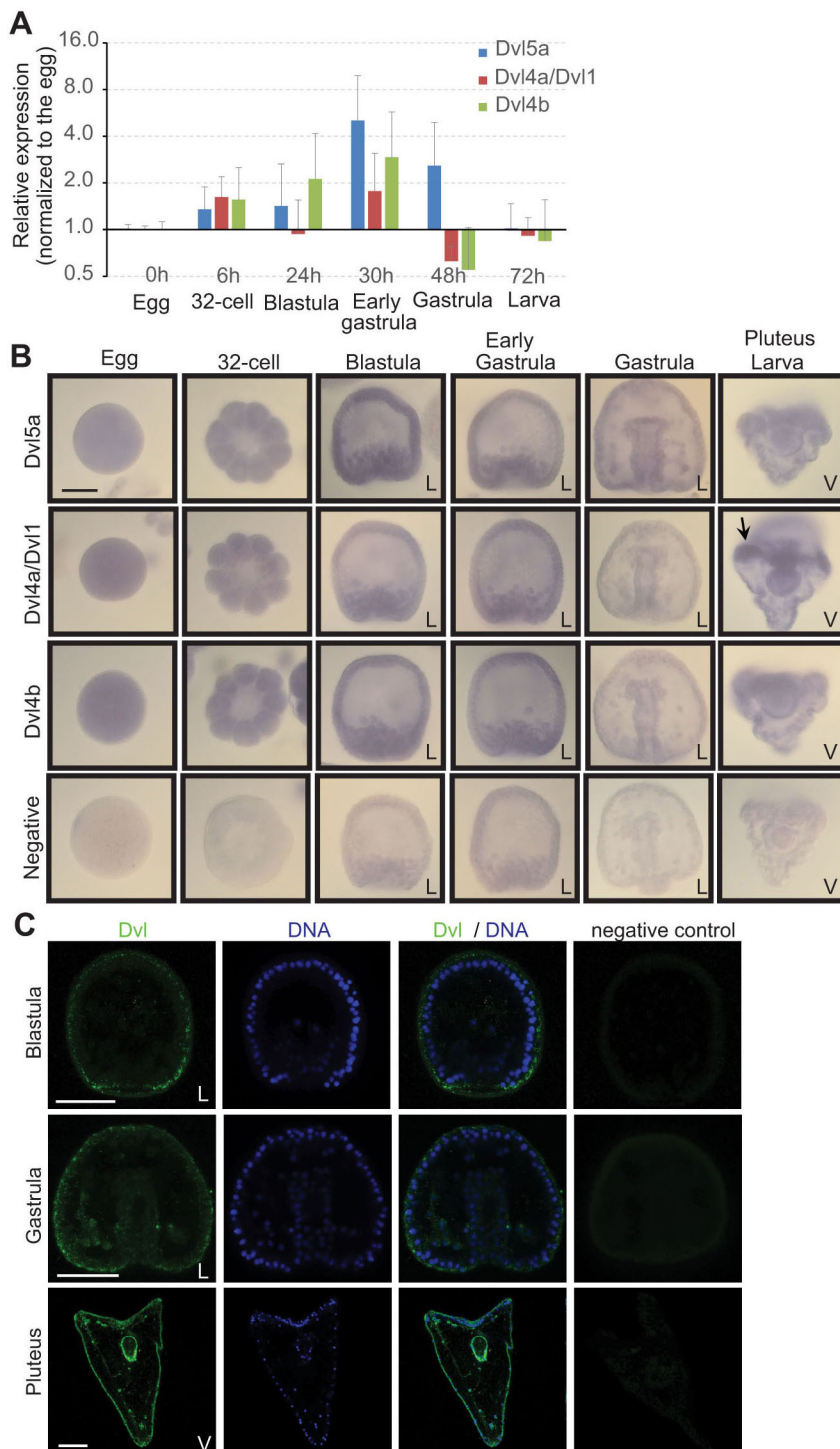


Fig. 2. Dvl isoforms are expressed during early embryogenesis.

(A) Two-hundred eggs or embryos were collected and subjected to QPCR analysis. At each developmental stage, there was no significant difference in gene expression compared with the egg stage ($P > 0.1$; Student's *t*-test). Each QPCR samples contains 100-200 embryos in 3-5 experimental replicates. (B) Embryos were hybridized with *Dvl* mRNA *in situ* probes. At the larval stage, distinct ciliary band staining (arrow) was observed in *Dvl4a/Dvl1*-labeled embryos. (C) Dvl proteins are expressed throughout development. From the blastula to gastrula stages, Dvl was enriched in the posterior end of the embryos. Dvl was also expressed in the gut and PMCs of gastrulae. At the larval stage, Dvl protein was enriched in the PMCs, endoderm, pyloric sphincter and ciliary band. Negative controls were embryos incubated with only the secondary antibody. L, lateral view; V, ventral view with ventral toward the top. Scale bars: 40 μ m (B); 50 μ m (C).

larval stage, Dvl protein was enriched in the gut, pyloric sphincter, PMCs and the ciliary band (Fig. 2C).

Dishevelled isoforms are directly suppressed by miRNAs

We bioinformatically identified 100% seed match of annotated sea urchin miRNAs within the 3'UTRs of all *Dvl* isoforms (Fig. 1B, Fig. 3A). To test the direct regulation of *Dvl5a*, *Dvl4a* and *Dvl4b* by these miRNAs, we cloned *Dvl* 3'UTRs downstream of *Renilla* luciferase (Rluc). Site-directed mutagenesis was used to alter the third and fifth base pairs of the seed sequences of *SpmiRDeep2-30364* and *SpmiR153** in *Dvl5a*; *SpmiRDeep2-30364*, *SpmiR2007* and *SpmiR2002* in *Dvl4a*; and *SpmiR200* in *Dvl4b* (Fig. 3A). Mutated seed sites would abolish endogenous miRNA binding to the target sites in the 3'UTR of these reporter constructs (Staton and Giraldez, 2011; Stepicheva et al., 2015). *In vitro*-transcribed mRNAs of *Rluc* fused to the wild-type or mutated *Dvl* 3'UTRs and the firefly reporter construct (used as a normalization control for *Rluc* luciferase) were co-injected into newly fertilized eggs (Stepicheva et al., 2015; Stepicheva and Song, 2015).

We collected injected mesenchyme blastulae and used dual luciferase assays to test direct miRNA suppression of these *Dvl* isoforms (Fig. 3B). The *Rluc* with mutated *SpmiRDeep2-30364* and *SpmiR153** seed sequences resulted in a significant increase of normalized luciferase signals compared with the *Rluc* with wild-type seed sequences, indicating that at least one of these miRNAs directly

suppress *Dvl5a* (Fig. 3B). For *Dvl4a*, *Rluc* fused with the 3'UTR with mutated seed sites for *SpmiRDeep2-30364*, *SpmiR2007* and *SpmiR2002* had significantly more luciferase signals compared with the *Rluc* fused with the wild-type 3'UTR, indicating that *Dvl4a* is directly suppressed by at least one of these miRNAs. We observed increased but not statistically significant *Rluc* signals from the *Dvl4b* construct with mutated *SpmiR200* seed sequence compared with the *Dvl4b* construct with wild-type 3'UTR, indicating that this miRNA may not be bona fide or plays a weak regulatory role. The overall relatively small increase in luciferase reading caused by the removal of miRNA suppression is consistent with the previous studies (Selbach et al., 2008; Nicolas, 2011; Stepicheva et al., 2015). These results indicate that *Dvl5a* and *Dvl4a* are directly suppressed by miRNAs.

Dvl miRNA target protector morpholinos (miRNATPs) modulate Dvl mRNA and protein levels

To test the impact of miRNA suppression of *Dvl* isoforms, we designed *Dvl* miRNATPs complementary to the miRNA regulatory binding sites of *Dvl5a* (*SpmiR153** at +230 bp), *Dvl4a* (*SpmiRDeep2-30364* and *SpmiR2002*) and *Dvl4b* (*SpmiR200*), as identified by bioinformatics analyses and luciferase assays (Fig. 1B, Fig. 3A). Zygotes were injected with a cocktail of three *Dvl* miRNATPs, each at 300 μ M, or control TP at 900 μ M. We then examined whether there were changes in the *Dvl* transcript and Dvl protein levels. Results indicated that *Dvl* miRNATP-injected

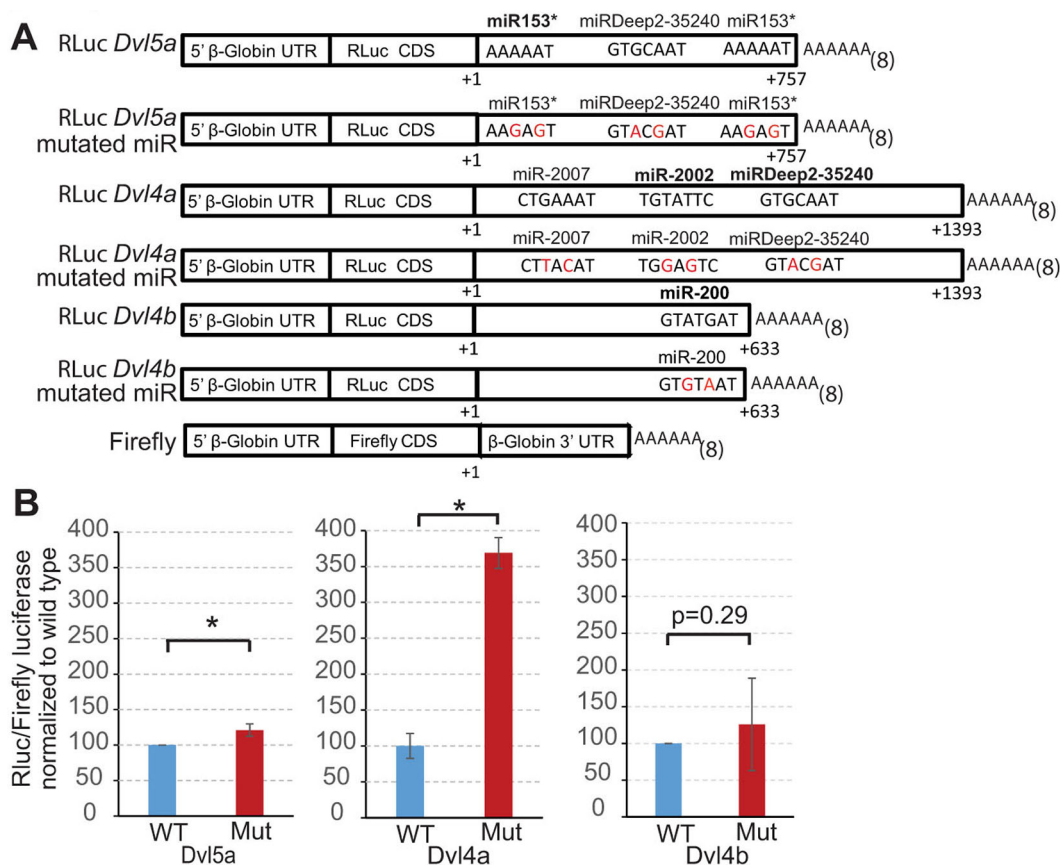


Fig. 3. miRNAs directly suppress *Dvl5a* and *Dvl4a*. (A) Unique 3'UTRs of various *Dvl* isoforms were cloned downstream of *Renilla* luciferase (Rluc). Site-directed mutagenesis was used to mutate selected seed sequences of predicted miRNA regulatory binding sites. *Dvl* miRNATPs were designed against specific miRNA-binding sites shown in bold in A (*miR153** of *Dvl5a*, *miR2002* and *miRDeep2-30364* of *Dvl4a*, and *miR200* of *Dvl4b*). Mutated residues are shown in red. (B) Firefly (control) and *Rluc* mRNAs were injected into newly fertilized eggs. Dual luciferase assays were conducted with mesenchyme blastulae at 24 hpf. *Dvl5a* and *Dvl4a* are directly suppressed by miRNAs. * $P < 0.05$. 3-5 experimental replicates were conducted. Each set contains 50 embryos. Mut, mutated seeds; WT, wild type.

embryos express *Dvl* isoforms and other components of the Wnt signaling pathway at similar levels compared with the controls (Fig. 4A). However, the transcript level of *Rac1*, which encodes a small GTPase that is downstream of the ncWnt/PCP pathway (Lindqvist et al., 2010), was significantly increased in *Dvl* miRNATP-injected embryos compared with control (Fig. 4A).

To test if blocking miRNA suppression of *Dvl* translation resulted in a change in Dvl, we immunolabeled control TP- and *Dvl* miRNATP-injected embryos at the 32-cell stage, when Dvl protein is enriched at the vegetal cortex (Peng and Wikramanayake, 2013). We took confocal z-stack images of these embryos and measured the total level of fluorescence pixels from Dvl immunolabeling. Results indicated that the *Dvl* miRNATP-injected embryos displayed an overall 1.5-fold increase of Dvl compared with the control TP-injected embryos (Fig. 4B,C). Interestingly, removal of specific miRNA suppression of *Dvl* isoforms resulted in an increase of ubiquitous Dvl protein throughout the embryo, as well as increased Dvl in the vegetal cortex.

Treatment with *Dvl* miRNATPs or *Dvl* mRNA results in dose-dependent aberrant gut morphology

Because the cWnt pathway is involved in endomesoderm specification, we examined the effect of blocking miRNA suppression of *Dvl* on the embryonic gut (Fig. 5). The sea urchin embryonic gut consists of a muscular esophagus (foregut), a large stomach (midgut) and a tubular intestine (hindgut) (Burke, 1981; Burke and Alvarez, 1988). Newly fertilized eggs were microinjected with *Dvl* miRNATPs against all three *Dvl* isoforms at various concentrations. We used the Endo1 antibody, which recognizes antigens of the mid and hindgut (Wessel and McClay, 1985), to examine the epithelial cell lining of the gut. Results indicated that 58% of *Dvl* miRNATP-injected embryos expressed

less Endo1 in the gut epithelium (the less severe phenotype) and 16% of the embryo failed to gastrulate (the more severe phenotype) (Fig. 5A).

Because blocking miRNA suppression of *Dvl* isoforms resulted in increased Dvl and various aberrant phenotypes, we overexpressed sea urchin *Dvl* isoforms to identify which phenotypes could be attributed to which *Dvl* isoform. We utilized the previously studied *LvDvl*, which has the sea urchin-specific C-terminus residues (YFDDSVSVTL), to examine the effect of *SpDvl4a/4b* overexpression. The *LvDvl* was modified to contain the conserved DEP-C residues that are shared by Dvl of other species, which we denoted as *LvDvl**, to resemble the *SpDvl5a* form (CEFFVDVM). These *Dvl* mRNAs were injected into zygotes. We found that overexpression of each isoform alone or in combination resulted in reduced Endo1 expression, in comparison with *mCherry* mRNA-injected control embryos (Fig. 5B), similar to the less severe gut phenotype of the *Dvl* miRNATP-injected embryos (Fig. 5A).

To evaluate gut morphology of the less severe gut phenotype of the *Dvl* miRNATP-injected embryos, we measured the width of the midgut and blastopore and calculated their ratios. Results indicated that in the highest dose of 300 μ M, the width of the midgut of *Dvl* miRNATP-injected embryos was significantly narrower and the blastopore was wider than the embryos injected with the control TP (Fig. 5C). Results indicated that overexpression with *LvDvl/SpDvl4a/4b*, *LvDvl*/SpDvl5a*, or *LvDvl/SpDvl4a/4b* plus *LvDvl*/SpDvl5a*, led to significantly wider blastopore width and narrower midgut, similar to the *Dvl* miRNATP-injected embryos (Fig. 5D).

Because we observed gut morphological differences in *Dvl* miRNATP-treated embryos, we tested whether endodermal differentiation was affected by examining expression of alkaline phosphatase (AP), which is an enzyme in the gut that is used as a differentiated endodermal marker (Fig. 5E) (Kumano and Nishida,

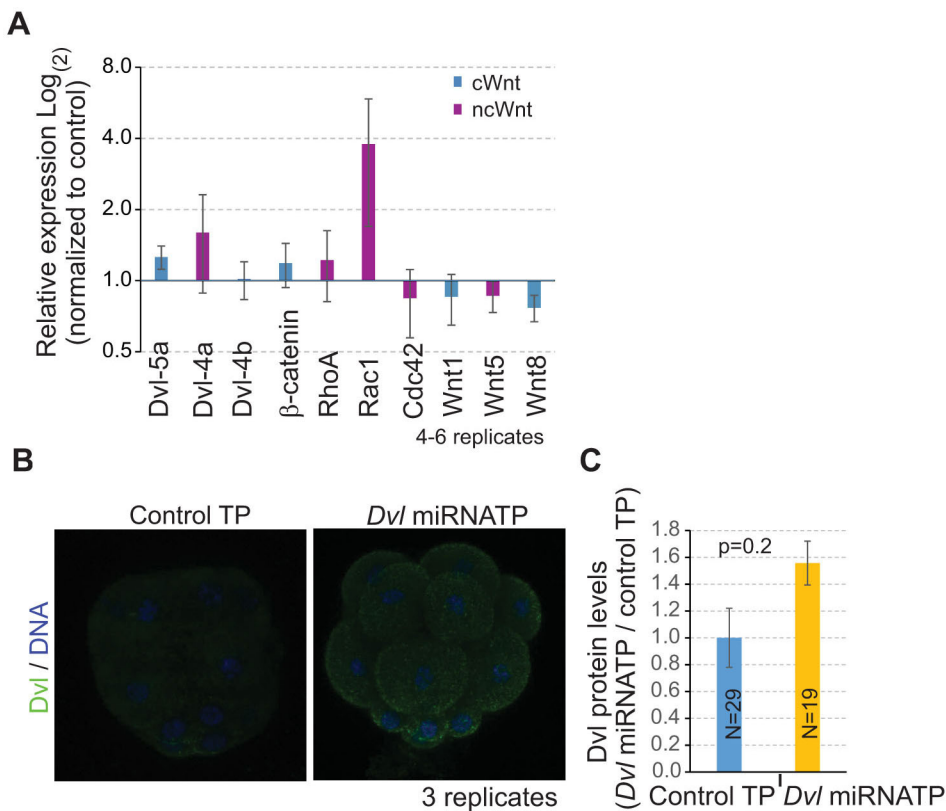


Fig. 4. Removing miRNA suppression of *Dvl* leads to increased *Rac1* expression and Dvl protein. (A) QPCR was used to measure transcriptional changes of genes in Wnt signaling pathways in control TP- and *Dvl* miRNATP-injected blastulae (300 μ M of each TP) at 24 hpf. *Rac1* increased by almost 4-fold. Designation of cWnt or ncWnt components are based on previous studies (Range et al., 2013; Cui et al., 2014; Minegishi et al., 2017) and this study. (B) 32-cell stage embryos were immunolabeled with Pan-Dvl antibody (green). Blue, Hoechst dye. (C) *Dvl* miRNATP-injected embryos had an overall increase in Dvl expression of 1.5-fold compared with control TP-injected embryos at the 32-cell stage. Confocal z-stack images were taken with scanning confocal microscopy. Fluorescence signals of maximum projections were quantified with Metamorph.

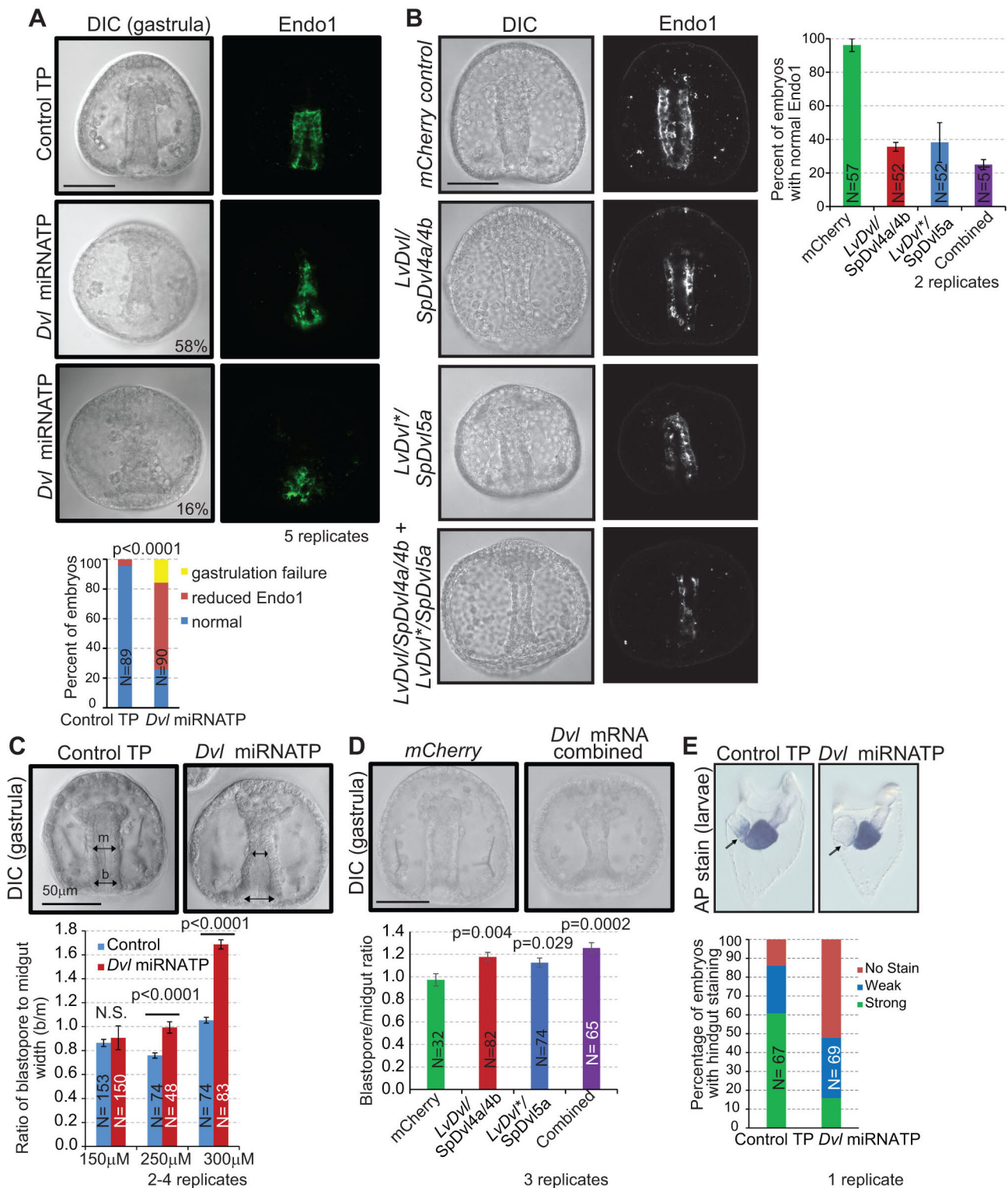


Fig. 5. *Dvl* isoform overexpression or removal of miRNA suppression of all *Dvl* isoforms results in aberrant gut morphology. (A,B) Gastrulae were immunolabeled with Endo1. *Dvl* miRNATP-injected embryos have either less Endo1 expression or gastrulation failure. *LvDvl/SpDvl4a/4b*-, *LvDvl*/SpDvl5a*-, and *LvDvl/SpDvl4a/4b* plus *LvDvl*/SpDvl5a*-injected embryos are either normal or exhibited less Endo1 expression. (C,D) In the embryos that had properly gastrulated, the ratio of the width of the blastopore (b) to the midgut (m) was significantly higher in *Dvl* miRNATP or *Dvl* mRNA (*LvDvl/SpDvl4a/4b* plus *LvDvl*/SpDvl5a*)-injected gastrulae compared with controls. (E) Control TP-injected embryos have more intense alkaline phosphatase (AP) staining in the hindgut compared with *Dvl* miRNATP-treated embryos (arrows). Scale bars: 50 μ m.

1998; Drawbridge, 2003). A significant number of *Dvl* miRNATP-treated larvae had little or no alkaline phosphatase activity present in the intestine (hindgut) compared with the control (Fig. 5E). These

results suggest that removing suppression of *Dvl* miRNAs resulted in *Dvl* protein increase that may negatively affect the function of the larval gut.

We investigated what might be the underlying molecular cause of these phenotypes in *Dvl* miRNATP-injected embryos by examining the spatial and quantitative expression of key transcription factors involved in endodermal specification. *Krl* and *FoxA* are expressed in the Veg2 cell lineage important for specifying the fore/midgut, and *Eve* and *Bra* are expressed in the Veg1 cell lineage important for hindgut specification (Peter and Davidson, 2011). The overall transcript levels of *Krl*, *FoxA*, *Eve* and *Bra* did not change in *Dvl* miRNATP- or combined *Dvl* mRNA (*LvDvl/SpDvl4a/4b* plus *LvDvl*/SpDvl5a*)-injected embryos compared with the control (Fig. 6A). However, the spatial expression domain of *Krl* was significantly decreased in *Dvl* miRNATP- or *Dvl* mRNA-injected embryos compared with controls (Fig. 6C). In addition, *Eve* exhibited a significant expansion of its spatial expression domain in *Dvl* miRNATP- or *Dvl* mRNA-injected embryos compared with controls (Fig. 6D). The spatial expression changes of key transcription factors involved in endodermal specification could result in changes in the gut morphology and potentially function of the gut.

Dvl mRNA overexpression and blockade of miRNA regulation of *Dvl* isoforms result in dose-dependent defects of skeletal spicules and PMC patterning

To test whether the removal of miRNA suppression of *Dvl* had an impact on skeletogenesis, newly fertilized eggs were microinjected with *Dvl* miRNATPs against all three *Dvl* isoforms at various concentrations. We observed a dose-dependent decrease of the dorsoventral connecting rods (DVCs) at gastrula stage (Fig. 7A). Injection of *Dvl* miRNATP at 300 μ M resulted in the most significant decrease of DVCs. In addition, results indicated that overexpression of *LvDvl/SpDvl4a/4b*, *LvDvl*/SpDvl5a*, or both together, resulted in a significant decrease in DVCs compared with the control, similar to *Dvl* miRNATP-injected embryos (Fig. 7B).

We also tested the PMC positioning in control TP- and *Dvl* miRNATP-injected embryos. We observed that embryos injected with 300 μ M of *Dvl* miRNATP had the most severe PMC defects with clustered PMCs at the sub-equatorial ring and a complete lack of anterior migration (Fig. 7C). The lower concentrations of *Dvl* miRNATP also resulted in some embryos with clustered

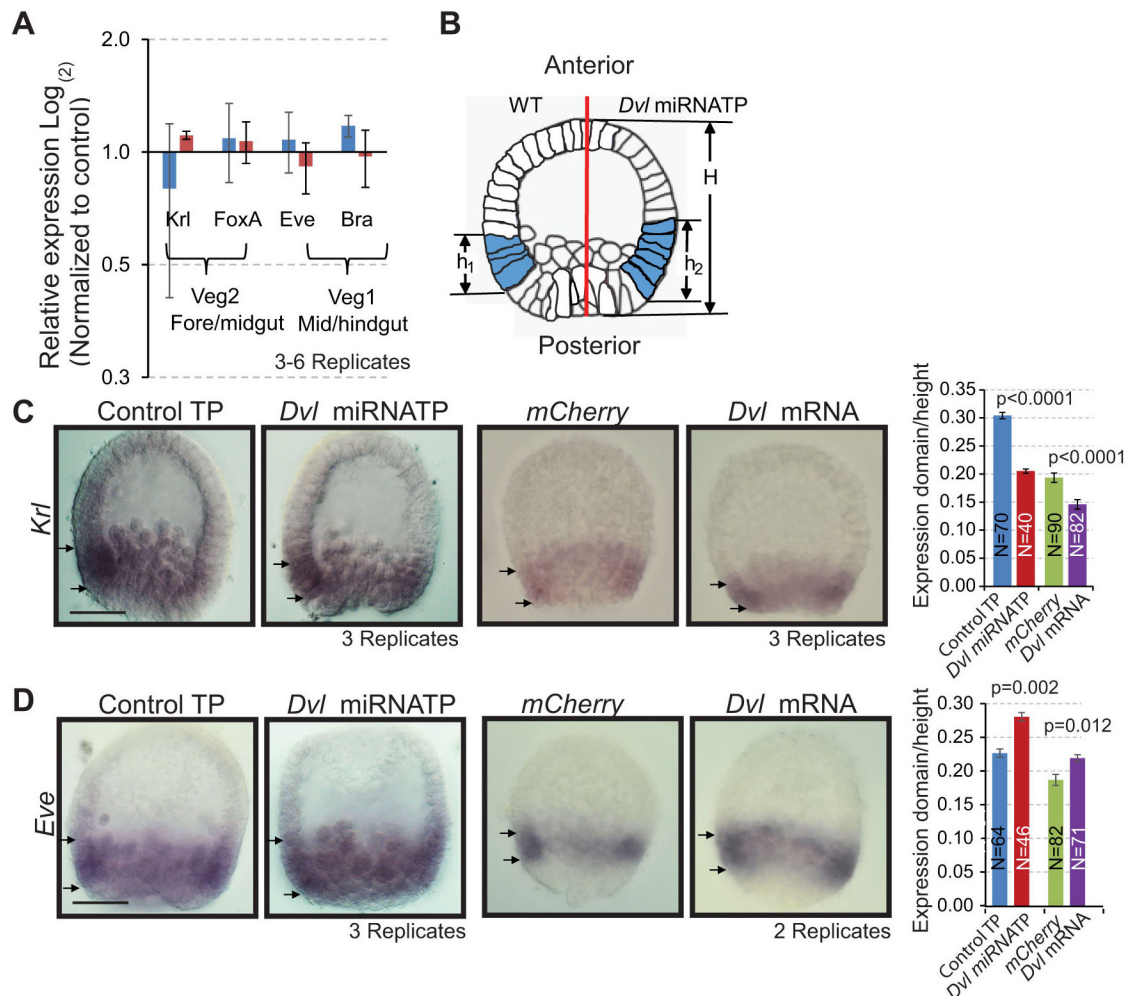


Fig. 6. *Dvl* mRNA overexpression or removal of miRNA suppression of *Dvl* isoforms results in decreased *Krl* spatial expression and expanded *Eve* spatial expression. (A) QPCR was used to measure transcriptional changes of Wnt-responsive endodermal genes in control TP- and *Dvl* miRNATP-injected embryos at 24 hpf. Overall transcript levels of *Eve*, *Bra*, *Krl* and *FoxA* did not change in *Dvl* miRNATP- or *Dvl* mRNA-injected embryos compared with control embryos. Blue is for *Dvl* miRNATP and red is for *Dvl* mRNA. (B) The expression domain is measured by taking the ratio of h_1 or h_2 to H . Red line indicates midline. (C) The expression domain of *Krl* is significantly decreased in *Dvl* miRNATP- or *Dvl* mRNA-injected embryos. (D) The spatial expression domain of *Eve* is significantly expanded in *Dvl* miRNATP- or *Dvl* mRNA-injected embryos. Lateral views shown. Scale bars: 40 μ m.

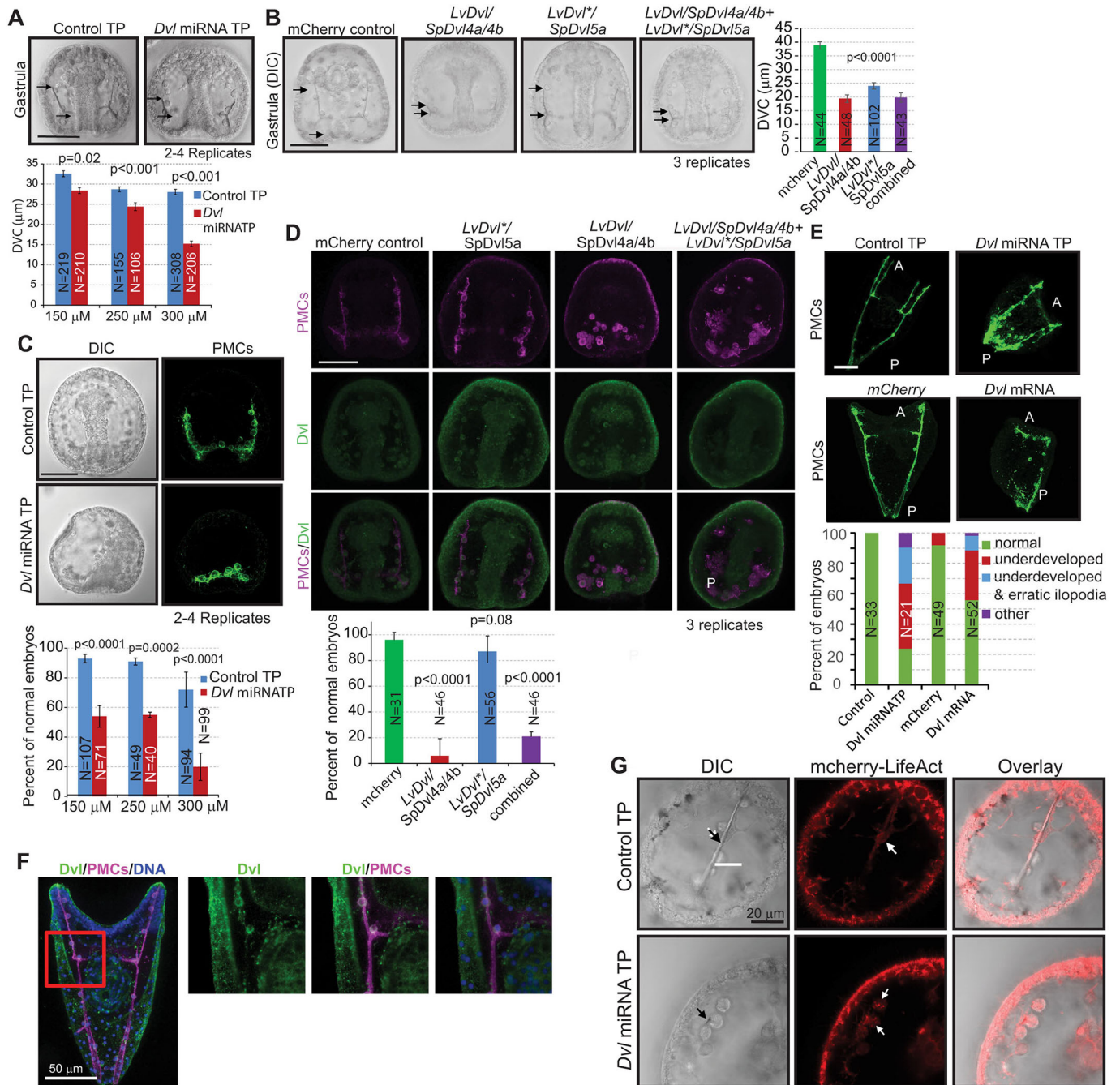


Fig. 7. *Dvl* mRNA overexpression or blockade of miRNA suppression of *Dvl* isoforms results in dose-dependent defects of spicule length and patterning of the PMCs. (A) *Dvl* miRNA TP-injected embryos displayed dose-dependent, shortened dorsoventral connecting rods (DVCs) in comparison with the control embryos. (B) *LvDvl/SpDvl4a/4b*-, *LvDvl*/SpDvl5a*-, and *LvDvl/SpDvl4a/4b* plus *LvDvl*/SpDvl5a*-injected embryos had shorter DVCs in comparison with *mCherry*-injected controls. Arrows indicate the length of the dorsoventral connecting rod (DVC). (C) PMCs were immunostained with the PMC-specific marker 1D5. *Dvl* miRNA TP-injected embryos displayed PMC clustering and lack of anterior migration in comparison with the control. (D) *LvDvl/SpDvl4a/4b*- and *LvDvl/SpDvl4a/4b* plus *LvDvl*/SpDvl5a*-injected embryos exhibited scattered and severe clustering of PMCs. (E) PMC defects persist to the larval stage (5 dpf), displaying PMC clustering and branched filopodia for both *Dvl* miRNA TP- and *LvDvl/SpDvl4a/4b* plus *LvDvl*/SpDvl5a*-injected embryos. A, anterior; P, posterior. (F) *Dvl* is expressed in PMCs and PMC connections. Embryos were collected at 5 dpf and immunolabeled with Pan-*Dvl* antibody (green), 1D5 to mark PMCs (magenta), and Hoechst dye to label DNA (blue). Red boxed area is enlarged on the right to show *Dvl* in PMCs. (G) Embryos were co-injected with *mCherry-LifeAct* to assay for actin in live gastrulae using scanning confocal microscopy. *Dvl* miRNA TP-injected embryos have punctate actin localization (white arrows) in presumptive PMCs clustered at the tri-radiate spicules (black arrow), whereas the presumptive PMCs along the long skeletal spicule in the control TP-injected embryos have more even actin distribution within these cells. Scale bars: 50 μm (unless indicated otherwise).

PMCs at the sub-equatorial ring, but PMCs were able to partially migrate anteriorly. Similarly, *LvDvl/SpDvl4a/4b* or *LvDvl/SpDvl4a/4b* plus *LvDvl*/SpDvl5a* co-injection resulted in scattered and clustered PMCs (Fig. 7D). No significant PMC

patterning defects were observed in embryos injected with the *LvDvl*/SpDvl5a* or in the *mCherry-LifeAct* mRNA-injected embryos, indicating that the *LvDvl/SpDvl4a/4b* isoform overexpression resulted in PMC patterning defects (Fig. 7D).

Importantly, the PMC patterning defects persisted into the larval stage 5 days post-fertilization (dpf), when the *Dvl* miRNATP-injected and *Dvl* mRNA (*LvDvl/SpDvl4a/4b* plus *LvDvl*/SpDvl5a*)-injected larvae exhibited clustered PMCs and branched filopodia (Fig. 7E). Interestingly, we found that *Dvl* is expressed in the PMCs, suggesting that PMCs themselves may be responsive to Wnt signaling activation (Fig. 7F).

To investigate further whether the failure of PMCs to migrate anteriorly might be due to defective motility, we co-injected *mCherry-LifeAct* mRNA with control TPs or *Dvl* miRNATPs into newly fertilized eggs to examine actin distribution. We observed that presumptive PMCs around the tri-radiate spicules of *Dvl* miRNATP-injected embryos have punctate actin localization, whereas the presumptive PMCs along the long skeletal spicules in the control TP-injected embryos had more even actin distribution within these cells (Fig. 7G). These results suggest that possible actin-remodeling defects might hinder proper PMC migration.

Dvl* mRNA overexpression or removal of miRNA suppression of *Dvl* results in decreased transcript levels of *Vegf3

To identify the underlying molecular mechanism that led to *Dvl* miRNATP- and *Dvl* mRNA-induced skeletal defects, we examined expressions of the following gene categories: (1) *Alx1*, which is essential for PMC specification (Ettensohn et al., 2003); (2) biomineralization genes *SM29*, *SM49*, *SM50* (Adomako-Ankomah and Ettensohn, 2013); (3) *Hnf6*, which regulates *SM50* (Otim et al., 2004; Otim, 2017); (4) factors that have been shown to be important for PMC positioning, including *Nodal*, *BMP2/4* (Yaguchi et al., 2008; Duboc et al., 2010), *Pax2/5/8* (Rottinger et al., 2008), *Vegf3* (Duloquin et al., 2007; Adomako-Ankomah and Ettensohn, 2013), *Alk2/4/7*, *Slc26a5* and *TGF- β rtII* (Piacentino et al., 2015, 2016; Sun and Ettensohn, 2017); and (5) *Kirrel*, which is involved in PMC fusion (Ettensohn and Dey, 2017) (Fig. 8A). Results indicated no significant expression difference for most genes tested, except for *Vegf3*, which had 50% of the transcripts in both *Dvl* miRNATP- and *Dvl* mRNA-injected embryos compared with control embryos. Previous literature indicated that the *Vegf3* signaling pathway provides guidance and differentiation cues to PMCs, as well as being crucial for forming skeletal elements (Duloquin et al., 2007; Adomako-Ankomah and Ettensohn, 2013).

We also examined the spatial expression of *Wnt5* and *Vegf3*. *Wnt5* acts as a short-range signal from the endoderm that activates the border ectoderm specification, which provides positioning cues for the PMCs (McIntyre et al., 2013). Results indicated that *Dvl* miRNATP-injected embryos did not have a significant change in the *Wnt5* expression domain, compared with the control TP-injected embryos. The spatial expression domain of *Vegf3* was significantly decreased in the *Dvl* miRNATP-injected or *Dvl* mRNA-injected embryos compared with controls (Fig. 8C). The expression domain of *VegfR10*, which encodes the cognate receptor for *Vegf3*, was unchanged and expressed in all PMCs in the *Dvl* miRNATP-injected, *Dvl* mRNA-injected, and control embryos (Fig. 8D).

***Dvl* mRNA overexpression or blockade of miRNA suppression of *Dvl* isoforms results in ciliary defects**

We noticed that *Dvl* miRNATP- and *Dvl* mRNA-injected larvae had swimming defects compared with the controls. The ciliary band arises after gastrulation and the ncWnt/PCP pathway has been

implicated in regulation of sea urchin ciliogenesis. Cilia are made up of microtubules consisting of tubulin subunits that enable the embryo to swim and feed (Yaguchi et al., 2010; Burke et al., 2014). To examine this swimming defect, we immunolabeled larvae with β -tubulin antibody to visualize cilia. The control TP-injected embryos had long, well projected cilia, whereas the *Dvl* miRNATP-injected larvae displayed aberrant apical and body cilia (Fig. 9A-C). The body cilia of *Dvl* miRNATP-injected embryos had kinks, whereas control TP-injected embryos cilia were long and curved (Fig. 9B). The apical cilia of the ciliary band in the *Dvl* miRNATP-injected larvae tend to be short, bent, sparse and disorganized compared with controls (Fig. 9A,C). To ensure that the aberrant morphology of the cilia in *Dvl* miRNATP-injected embryos was not due to fixation artifacts, we also examined cilia in living larvae. We observed that both apical and body cilia in *Dvl* miRNATP-injected embryos were bent with irregular beating compared with the control TP-injected embryos, which had long cilia with synchronous beating (Movies 1-4).

Similar to the *Dvl* miRNATP-injected embryos, overexpression of *LvDvl/SpDvl4a/4b*, *LvDvl*/SpDvl5a*, or both, resulted in bent ciliary defects compared with the long, protruding cilia of *mCherry* mRNA-injected control larvae (Fig. 9D, Movies 5-8).

DISCUSSION

Dishevelled is an important protein in the Wnt signaling pathway that plays a significant role in relaying cellular information to various developmental pathways (Gao and Chen, 2010). We identified several miRNAs that suppress different isoforms of *Dvl* and revealed that post-transcriptional regulation of *Dvl* is crucial for proper development. Furthermore, blockade of miRNA suppression of *Dvl* isoforms induced defects in the gut, spiculogenesis and ciliogenesis. These developmental defects of *Dvl* miRNATP-injected embryos are mimicked by the overexpression of *Dvl* isoforms. Developmental defects in *Dvl* miRNATP- and *Dvl* mRNA-injected embryos are likely to be due to perturbation of Wnt signaling pathways, as well as other *Dvl* functions in the embryo.

Dvl is ubiquitously expressed and highly enriched at the vegetal pole of early embryos (Peng and Wikramanayake, 2013). By blocking miRNA suppression of *Dvl* isoforms, we observed a 1.5-fold increase of the *Dvl* protein (Fig. 4B,C). This may be an underestimate, because we did not block all potential miRNA regulatory sites. Of note is that each *Dvl* miRNATP is complementary to the specific miRNA's seed sequence (6 bp) and the unique *Dvl* 3'UTR sequences flanking the miRNA seed sequence (additional 19 bp). Thus, each *Dvl* miRNATP uniquely targets that specific miRNA seed site within the particular *Dvl* isoform. We found that *Dvl* is increased in the entire *Dvl* miRNATP-injected 32-cell embryos with enhanced enrichment in the vegetal pole of the embryo compared with control TP-injected embryos. This suggests that the miRNAs we identified play a role in suppressing *Dvl* throughout the embryo. Furthermore, the increase in *Dvl* protein induced by *Dvl* miRNATP was dose dependent, indicating specificity of the miRNATPs (Fig. 4B,C, Fig. S2A).

All miRNAs that are predicted to bind to *Dvl* isoforms are present throughout development (Fig. S3). Interestingly, miRDeep2-30364, one of the miRNAs that may suppress sea urchin *Dvl5a* and *Dvl4a*, also suppresses the sea urchin β -catenin (Stepicheva et al., 2015). Previously, we have shown that miRDeep2-30364 and miR2007 directly suppressed β -catenin and resulted in increased gene expression of downstream cWnt-responsive transcription factors, including *Eve*, *Bra*, *Krl* and *FoxA* (Stepicheva et al., 2015). This is

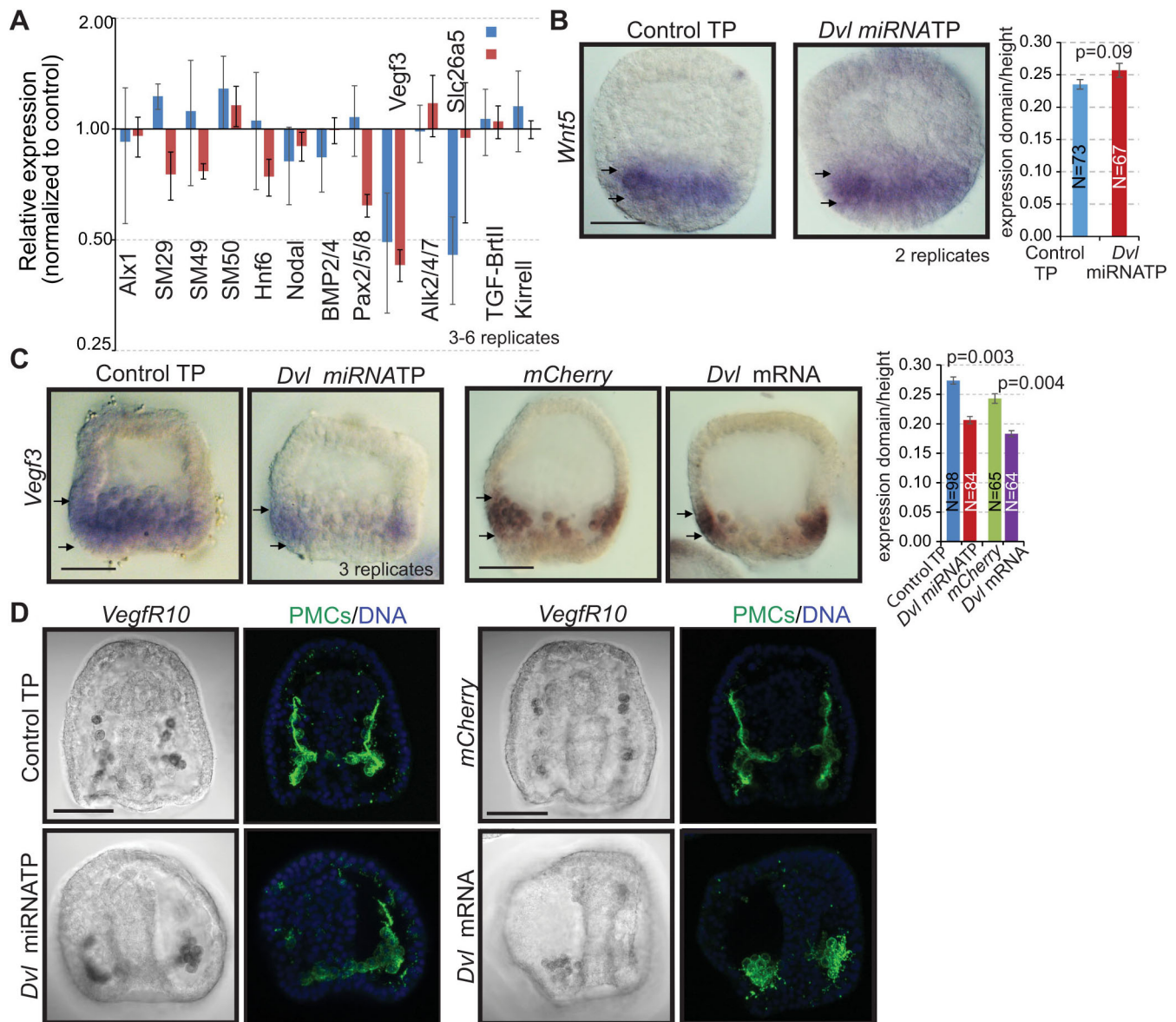


Fig. 8. *Dvl* overexpression or removal of miRNA suppression of *Dvl* results in decreased *Vegf3* expression. (A) QPCR was used to measure transcriptional changes of genes involved in PMC development and function in *Dvl* miRNATP-, *Dvl* mRNA (*LvDvl/SpDvl4a/4b* plus *LvDvl/SpDvl5a*)-injected embryos and controls at 24 hpf. *Dvl* miRNATP- or *Dvl* mRNA-injected embryos have 50% less transcripts compared with controls. Blue is for *Dvl* miRNATP and red is for *Dvl* mRNA. (B) *Wnt5* has a slightly expanded spatial expression domain compared with controls at 15 hpf. (C) *Vegf3* spatial expression domain is significantly decreased in the *Dvl* miRNATP- or *Dvl* mRNA-injected embryos compared with their corresponding controls. Arrows in B and C indicate expression domains of *Wnt5* and *Vegf3*, respectively. (D) *VegfR10* expression is not altered in the *Dvl* miRNATP- or *Dvl* mRNA-injected embryos compared with controls. $n=21$ –32 embryos in one replicate. Scale bars: 50 μ m.

typical of miRNA function as individual miRNAs often target multiple genes in the same developmental pathway (Stepicheva and Song, 2015).

Because we introduced *Dvl* miRNATP against at least one miRNA in all *Dvl* isoforms, we expected that elevation of *Dvl* protein would lead to the disassembly of the destruction complex and increase levels of β -catenin, which is a key effector protein of the cWnt pathway. β -Catenin enters the nuclei of vegetal blastomeres where it regulates endomesoderm specification (Weitzel et al., 2004). Our laboratory previously found that blocking miRNA suppression of β -catenin resulted in increased β -catenin and induced aberrant gut morphology (Stepicheva et al., 2015). Similarly, here we observed that *Dvl* miRNATP- or *Dvl* mRNA-injected embryos had significantly narrower midguts

compared with control embryos (Fig. 5A,B). This is consistent with our observation that *Dvl* is localized to the gut and in the pyloric sphincter of larvae (Figs 2 and 9).

Whereas cWnt is important for gut development, ncWnt may contribute to the wide blastopore phenotype in the *Dvl* miRNATP- or *Dvl* mRNA-injected embryos. In *Xenopus*, manipulations of *Dvl* through injections of dominant-negative mutant *Xdsh* (*Xdd1*), which has an internal deletion of the conserved PDZ domain, led to disruptions of ncWnt/PCP genes and resulted in failure of blastopore to close (Sokol, 1996; Ewald et al., 2004). Also in *Xenopus*, overexpression of a core PCP gene, *Strabismus* (*Stbm*), or deletion of a crucial regulator of ncWnt/PCP, NEDD4L, both resulted in delayed blastopore and neural tube closing (Darken et al., 2002; Zhang et al., 2014).

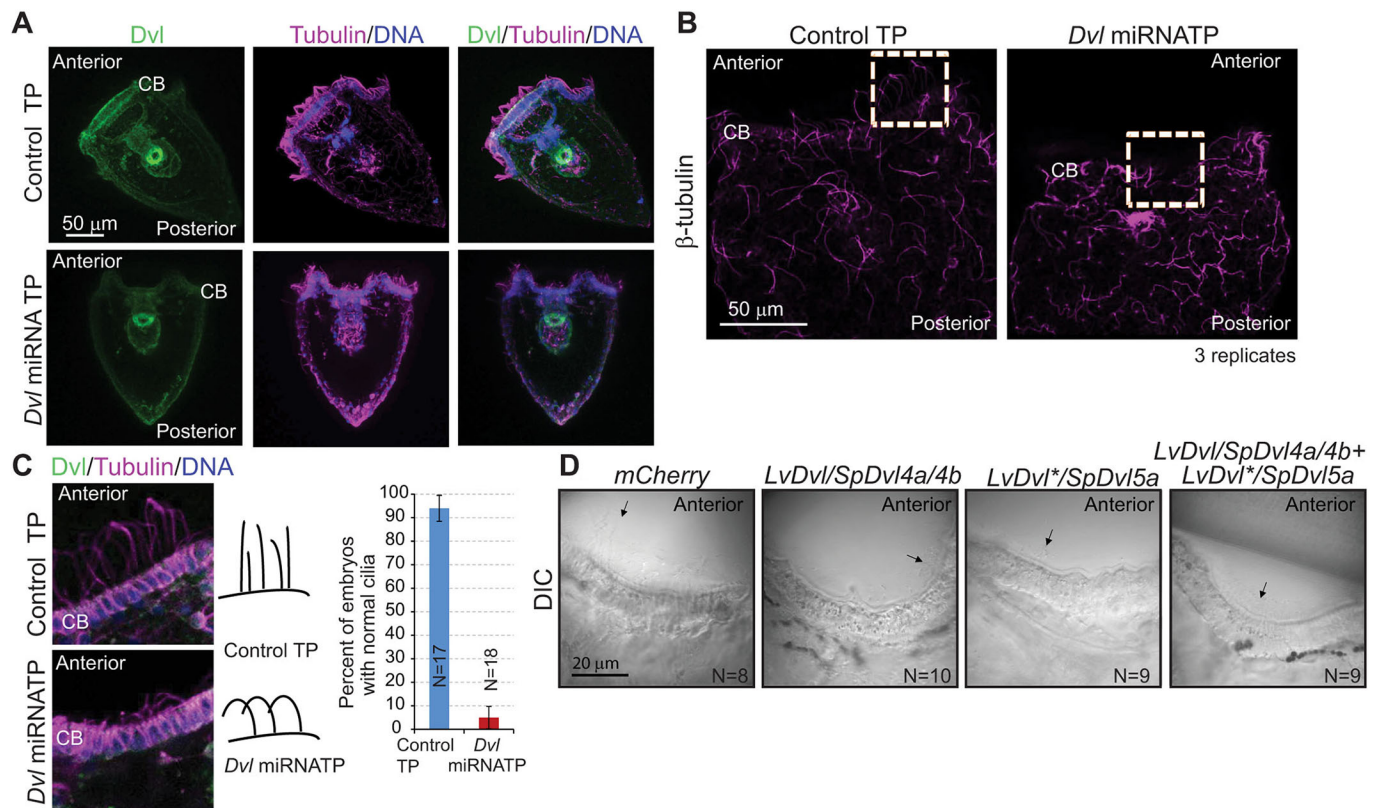


Fig. 9. *Dvl* overexpression or removal of miRNA suppression of *Dvl* isoforms results in shorter and aberrantly structured cilia.

(A–C) Embryos were collected at 5 dpf and immunolabeled with Pan-*Dvl* antibody (green), β -tubulin antibody (magenta) and Hoechst dye (blue) against DNA. (B) The epithelial cilia in the anterior larval body were imaged. *Dvl* miRNATP-injected embryos have kinks in body cilia compared with control embryos. (C) *Dvl* miRNATP-injected embryos had shorter cilia in bent orientation in the ciliary band compared with controls. CB, ciliary band. Images are magnifications of the boxed areas in B. (D) Live imaging of *Dvl* mRNA-injected larvae indicated similar ciliary defects as observed in *Dvl* miRNATP-injected larvae.

Another indication that *Dvl* miRNATP-injected embryos have potential gut function defects is that they have much less AP staining in the hindgut (Fig. 5E). In sea urchin larvae, AP is expressed only in differentiated endoderm (Whittaker, 1990; Kumano and Nishida, 1998; Drawbridge, 2003). These results indicate that both the morphology and potentially the function of the gut are negatively impacted by increased *Dvl*, induced by blocking miRNA-mediated post-transcriptional suppression of *Dvl*.

To reveal the molecular mechanism of *Dvl* miRNATP- or *Dvl* mRNA-induced gut phenotypes, we assayed for changes in transcription factors important for endodermal specification (Fig. 6). Canonical Wnt/ β -catenin signaling activates endodermal regulatory genes, such as *Krl* and *Eve*, to give rise to the foregut, midgut and hindgut (Howard et al., 2001; Peter and Davidson, 2010, 2011). We observed a significant decrease in the spatial expression domain of *Krl* and a significant increase in the expression domain of *Eve* in *Dvl* miRNATP- and in *Dvl* mRNA-injected embryos compared with controls (Fig. 6C–F). These results provided independent evidence that increased *Dvl* leads to expression changes in *Krl* and *Eve* (Fig. 6). *Krl* knockdown in the sea urchin blocks endoderm differentiation and results in failed gastrulation (Howard et al., 2001; Yamazaki et al., 2008). Thus, a moderate decrease in *Krl* expression domain may impact endoderm differentiation and gastrulation. *Eve* is directly activated by Wnt/ β -catenin, Hox11/13b and *Eve* itself (Peter and Davidson, 2011). In the intermediate germ cricket, *Gryllus bimaculatus*, *Krl* RNAi resulted in elimination of some *Eve*-regulated segmental stripes, suggesting that *Krl* is involved in the formation of those stripes by

regulating *Eve* (Mito et al., 2006). However, *Krl* morpholino knockdown in the sea urchin had no effect on *Eve* expression in the early blastula stage (18 hpf). Conversely, *Eve* morpholino knockdown had a small effect on *Krl* expression, indicating that they are not likely to regulate each other (Peter and Davidson, 2010). Nonetheless, the decreased expression domain of *Krl* and the increased *Eve* expression domain induced by *Dvl* miRNATPs or *Dvl* mRNA overexpression may contribute to the gut morphology and developmental defects we observed.

Blockade of miRNA suppression of *Dvl* isoforms resulted in dose-dependent defects in skeletal spicules and PMC patterning (Fig. 7). We also observed *Dvl* miRNATP- or *Dvl* mRNA-induced embryos have 50% less *Vegf3* expression and decreased *Vegf3* expression domain compared with controls (Fig. 8A,C). *Dvl* mRNA-induced gene expression changes and PMC defects are likely to be specific, as a lower dosage of *Dvl* mRNA-injected embryos did not result in these changes (Fig. S2B). However, we cannot distinguish direct versus indirect effects of *Dvl* mRNA overexpression-induced phenotypes. PMCs undergo a series of directed movements whereby their patterning is in part in response to the Vegf signaling pathway (Duloquin et al., 2007; Adomako-Ankomah and Etensohn, 2013). PMCs express the VegfR10 receptor; binding of its ligand, Vegf3, which is expressed in the ectoderm, guides the PMCs to migrate anteriorly, as well as providing differentiation cues to the PMCs. Vegf3 also regulates the expression of many biomineralization genes in the PMC gene regulatory network (Adomako-Ankomah and Etensohn, 2013). Loss of the VegfR10 receptor or Vegf3 results in PMCs that fail to

pattern and do not secrete a skeleton (Adomako-Ankomah and Ettensohn, 2013; Duloquin et al., 2007). We did not detect expression changes of *VegfR10* in *Dvl* miRNATP- or *Dvl* mRNA-injected embryos (Fig. 8D). The decrease in *Vegf3* level and expression domain may in part explain the *Dvl* miRNATP- and *Dvl* mRNA-induced skeletal and patterning defects of the PMCs.

Another potential contributor to the PMC patterning defect in *Dvl* miRNATP-injected embryos may be defects in PMC motility. As ncWnt mediates cell polarity and actin polymerization, increased Dvl may misregulate cell motility mediators, resulting in defective PMC motility. We found that Dvl protein is expressed in the PMCs, suggesting that Dvl may activate the ncWnt pathways or Wnt-independent functions in mediating cell motility of PMCs (Fig. 7G). To investigate this further, we examined the transcript levels of *RhoA*, *Rac1* and *Cdc42* downstream of the ncWnt/PCP pathways in *Dvl* miRNATP-injected and control embryos. We found that *Rac1* transcript levels were elevated in *Dvl* miRNATP-injected embryos by almost 4-fold (Fig. 4A). Because Rac1 regulates actin polymerization (Chung et al., 2000), we used an *mCherry-LifeAct* reporter, which encodes a 17 amino acid peptide that binds to filamentous actin (Riedl et al., 2008), to examine actin dynamics in the early embryo. We observed more punctate actin structures in the *Dvl* miRNATP-injected presumptive PMCs compared with the control (Fig. 7H). In chicken embryo fibroblasts, overexpression of Rac proteins induced disassembly of existing F-actin-containing stress fibers, which consist of long, highly branched bundled actin-rich protrusions, that resulted in dramatic changes in cell morphology (Albertinazzi et al., 1999). The punctate actin structures in *Dvl* miRNATP-injected embryos may indicate defective actin polymerization, contributing to the inability of PMCs to migrate properly.

These PMC patterning defects are not likely to be acting on the cWnt signaling pathway, as our previous study indicated that removing miRNA suppression of β -catenin had no impact on PMC patterning (Stepicheva et al., 2015). In addition, the overexpression of the *LvDvl/SpDvl4a/4b* resulted in significantly shorter DVCs and in PMC patterning defects (Fig. 7B,D). These results indicated that the skeletal and PMC defects observed in the *Dvl* miRNATP-injected embryos are likely to be due to the increased *SpDvl4a/4b* isoform. The molecular mechanism of how *Dvl4a/4b* regulates skeletogenesis remains unclear.

An unexpected and interesting finding is that *Dvl* miRNATP-, *LvDvl/SpDvl4a/4b*- and *LvDvl*/SpDvl5a*-injected embryos all had swimming and ciliary defects (Fig. 9, Movies 1-8). Sea urchins have motile monocilia on their ectodermal cells that allow the embryos and larvae to swim with coordinated ciliary beating and to feed (Kinukawa and Vacquier, 2007; Mizuno et al., 2017). A previous study indicated that Dvl-DEP overexpression resulted in embryos that failed to swim (Byrum et al., 2009). The swimming defect observed in *Dvl* miRNATP- and *Dvl* mRNA-injected embryos may result from improper ciliary coordination; the direction of ciliary movement depends on the orientation of the basal body, which is primarily determined by the PCP pathway (Marshall and Kintner, 2008; Kunitomo et al., 2012; Mizuno et al., 2017). Dvl in *Xenopus* is found at the base of the cilia and is essential for apical positioning of the basal bodies and positioning of cilia (Park et al., 2008; Mlodzik, 2016). Knockdown of *Dvl1* and *Dvl3* in *Xenopus* and knockdown of *Stbm* in *Clytia* resulted in phenotypes of fewer and shorter cilia (Park et al., 2008; Momose et al., 2012), indicating that Dvl plays an evolutionarily conserved role in proper cilia formation. PCP signaling plays a crucial role in ciliogenesis; however, the Wnt/ β -catenin also regulates ciliogenesis via *foxj1a* expression in zebrafish Kupffer's vesicle. Downregulation of cWnt/ β -catenin

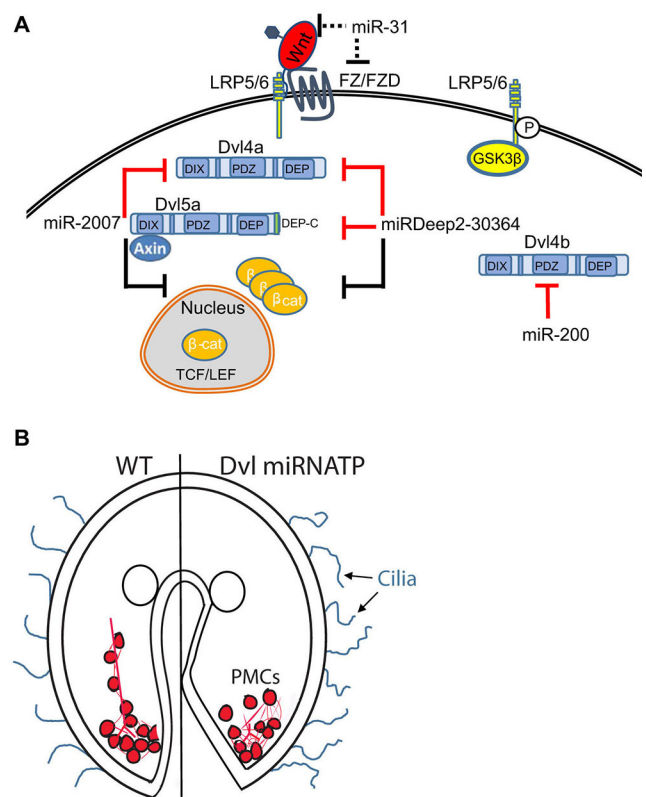


Fig. 10. Post-transcriptional regulation of the Wnt signaling components by miRNAs. (A) Schematic summarizing current knowledge of sea urchin miRNAs that regulate Wnt signaling components (Stepicheva et al., 2015; Stepicheva and Song, 2015). Red lines indicate findings from the current study. Black lines represent results from our previous studies. (B) Schematic illustrating the gut, PMC and ciliary defects induced by removal of miRNA suppression of *Dvl* isoforms. WT, wild type.

leads to depletion of Lef1 and Tcf7, inhibiting *foxj1a* transcription. This results in shorter and fewer cilia with loss of cilia motility that can be rescued with overexpression *foxj1a* (Lin and Xu, 2009; Caron et al., 2012; Zhu et al., 2015). Dvl has also been shown to interact with DCDC2, which binds to tubulin to enhance microtubule polymerization and localizes to the ciliary axoneme (Schueler et al., 2015). Wnt inhibitor treatment rescued the effects of *dcdc2* knockdown-induced ciliopathy in renal spheroid cells and zebrafish embryos, suggesting that cWnt signaling is involved in the process of ciliation (Schueler et al., 2015). Thus, the ciliary defect observed in *Dvl* miRNATP-injected embryos may result from perturbations of both the ncWnt/PCP and the cWnt pathways.

Conclusions

This study demonstrated that miRNAs suppress various *Dvl* isoforms in the sea urchin embryo. We have shown that Wnt signaling pathway components are controlled post-transcriptionally by miRNAs (Fig. 10). Importantly, the level of increased Dvl protein, induced by blocking miRNA-mediated suppression of *Dvl* isoforms, is sufficient to induce various defects in the gut, spiculogenesis and ciliogenesis during development.

MATERIALS AND METHODS

Animals

Adult *Strongylocentrotus purpuratus* were obtained from Point Loma Marine Invertebrate Lab, Lakeside, CA, USA. Adult males and females

were given 0.5 M KCl intracoelomic injections for obtaining sperm and eggs. Filtered natural sea water (collected from Indian River Inlet; University of Delaware, DE, USA) or artificial seawater was used for embryo cultures incubated at 15°C.

Whole-mount *in situ* hybridization

Krl, *Eve*, *Wnt5* and *Vegf3* were cloned into Blunt-TOPO vectors (Thermo Fisher Scientific) (Stepicheva et al., 2015; Stepicheva and Song, 2015). *Krl*, *Eve*, *Wnt5* and *Vegf3* were linearized with restriction enzymes *Eco*RI, *Eco*RI, *Nor*I and *Bam*HI, respectively. All were *in vitro* transcribed with Sp6 RNA polymerase, except for *Vegf3* which was *in vitro* transcribed with T7 RNA polymerase using the DIG RNA Labeling Kit (Sigma-Aldrich). *Dvl5a* and *Dvl4b* 3'UTRs were synthesized as gBlock DNA fragments from IDTna.com (Integrated DNA Technologies) and cloned into Blunt-TOPO vectors. *Dvl4a* 3'UTR was PCR amplified with *Dvl4a* (For 5'-GGCCTC-GAGAGTGC GGAAATTTTGAATCAT-3'; Rev 5'-GGCGCGGCCG-CAATAATGACCGCTCAATTTT-3') and cloned into Blunt-TOPO vectors. *Xho*I and *Nor*I cut sites are underlined. All *Dvl* probes are linearized with *Nor*I and *in vitro* transcribed with Sp6 RNA polymerase. All *Dvl in situ* hybridizations were examined in 180-300 embryos for each stage in three to eight experimental replicates.

Cloning of luciferase reporter constructs

For generating *Dvl* 3'UTR luciferase reporter constructs, *Dvl5a* and *Dvl4b* 3'UTR was synthesized as a gBlock DNA fragment (Integrated DNA Technologies). *Dvl4a* 3'UTR in Blunt-TOPO was subcloned into the *Renilla* luciferase construct. All seed sequences were mutated at positions 3 and 5 within the miRNA seed sequences (Gregory et al., 2008; Stepicheva et al., 2015). *SpmiRDeep2-30364* was modified from 5'-GUGCAAU-3' to 5'-GUACGAU-3'; *spu-miR-153** was modified from 5'-AAAAAT-3' to 5'-AAGAGT-3'; *SpmiR2002* was modified from 5'-CTGAAAT-3' to 5'-CTTACAT-3'; *SpmiR2007* was modified from 5'-CTGAAAT-3' to 5'-CTTACAT-3'; and *SpmiR200* was modified from 5'-GTATGAT-3' to 5'-GTGTAAT-3'. Mutated nucleotides are underlined. All positive clones were identified by DNA sequencing (Genewiz). Firefly luciferase was used as loading control as previously described (Stepicheva et al., 2015). Luciferase constructs containing the *Dvl* 3'UTRs were linearized with *Eco*RI and *in vitro* transcribed using the mMessage machine kit with either T7 (for *Dvl* mRNAs) or Sp6 (for firefly luciferase mRNAs) RNA polymerases (Ambion) according to the manufacturer's instructions. mRNAs were purified by using the Macherey-Nagel Nucleospin RNA Clean-up kit according to the manufacturer's instructions. *In vitro*-transcribed mRNAs were loaded onto the Millipore spin columns to further clean the mRNAs prior to injections.

Cloning of *LvDvl**

To identify the contribution of *Dvl* isoforms to *Dvl* miRNATP phenotypes, we injected mRNA coding for two *Dvl* isoforms into zygotes. *LvDvl* protein is 93% identical to *SpDvl4a/4b*. The sea urchin species *L. variegatus* diverged from *S. purpuratus* about 50 million years ago. These two sister species of sea urchin have many similarities at the genomic as well as at the gene regulatory levels (Crain and Bushman, 1983; Ettensohn et al., 2004). Because of the relatively close evolutionary distance of *L. variegatus* to *S. purpuratus* and their high protein identity especially at the C-terminus of the protein, we used the available *LvDvl* clone (Weitzel et al., 2004) to represent the *SpDvl4a/4b* protein (Fig. 1). Because of the difficulty of cloning the *SpDvl5a* isoform, we used PCR to replace the sequence coding for the amino acids YFDDSVSVTLL in *LvDvl* to a sequence coding for the highly conserved CEFFVDVM amino acid sequence. Because the goal was to test whether overexpression of *SpDvl* isoforms would induce phenotypes similar to *Dvl* miRNATPs-injected embryos, we did not add the endogenous 3'UTRs to these protein coding sequences. Thus, *LvDvl* was used to mimic *SpDvl4a/4b* (denoted as *LvDvl/SpDvl4a/4b*) and *LvDvl+ CEFFVDVM* was used to mimic *SpDvl5a* (denoted as *LvDvl*/SpDvl5a*). To obtain *LvDvl**, the *LvDvl:Flag* construct was modified using Q5 Site-Directed Mutagenesis Kit (NEB). Primers used to change the amino acids YFDDSVSVTLL on the C terminus of *LvDvl:Flag* to CEFFVDVM were: For 5'-GTCGATGTCATGTGAATTCAAGGCCTCTCG-3' and Rev 5'-

AAAGAACTCACAAGGGTTTCCCATAGCCAT-3'. The Flag tag region was deleted after mutation. Plasmids were sequenced to verify that correct mutations were introduced. These plasmids were *in vitro* transcribed and mRNA coding for the two *Dvl* isoforms were injected into zygotes.

Microinjections

Microinjections were performed as previously described with modifications (Cheers and Ettensohn, 2004; Stepicheva and Song, 2014). For luciferase assays, 100 ng of *Renilla* luciferase and 60 ng of firefly luciferase were prepared in 2.5 µl of injection solution consisting of 0.5 µl 100% glycerol and 0.5 µl Texas Red dextran (Molecular Probes). Approximately 1-2 pl was injected into each newly fertilized egg. The stock injection solution contained 150, 250 or 300 µM of each *Dvl* miRNATP or 450, 750 or 900 µM of control TP in 20% sterile glycerol, 2 mg/ml 10,000 MW Texas Red lysine charged dextran (Molecular Probes) (as previously described; Stepicheva et al., 2015; Stepicheva and Song, 2015). For *Dvl* miRNATPs, we blasted each of the *Dvl* miRNATPs against the annotated sea urchin genome and identified them to be complementary to only the *Dvl* genes. Each *Dvl* miRNATP is complementary to the miRNA's seed sequence (6 bp) and the unique *Dvl* 3'UTR sequences flanking the miRNA seed sequence. Thus, each *Dvl* miRNATP is uniquely targeting that specific miRNA seed site within the particular *Dvl* isoform. We microinjected zygotes with a cocktail of *Dvl* miRNATPs corresponding to miR153* at position +230 of *Dvl5a* (5'-CTAGCATTTTTTTTTTGAAGCTGT-3'), to miR-2002 and miR-Deep2-35240 at positions +1198 and +1224 of *Dvl4a* (5'-TTGCACTTCATGATGCATAGAATAC-3') and to miR-200 at position +219 of *Dvl4b* (5'-ATTAATATCATACCCAAAACATATT-3') at 300 µM each or 900 µM of the negative control (5'-CCTCTTACCTCAGTTACAA-TTTATA-3') that corrects a splicing error of the human β-globin pre-mRNA (Kang et al., 1998).

To examine the actin dynamics in control TP and *Dvl* miRNATP, we microinjected newly fertilized eggs with 500 ng mCherry-LifeAct reporter mRNA, 0.5 µl 100% glycerol and 0.5 µl of Texas Red in a 2.5 µl injection solution (Riedl et al., 2008; Stepicheva et al., 2017).

To identify the impact of individual *Dvl* isoforms, *LvDvl/SpDvl4a/4b* mRNA, encoding the sea urchin-specific form of *Dvl* ending with YFDDSVTLL, and *LvDvl*/SpDvl5a* mRNA modified to contain the conserved DEP-C domain (CEFFVDVM), were injected into newly fertilized eggs. Stock injection solutions of 2.5 µl consisted of 0.5 µl 100% glycerol, 2.5 µg *LvDvl/SpDvl4a/4b* or *LvDvl*/SpDvl5a* or combinations of both (each with 1.25 µg of mRNA), with 500 ng of mCherry mRNA. The control solution contained 500 ng of mCherry without *Dvl* mRNA.

Dual luciferase quantification

All dual luciferase quantification was performed using the Promega Dual-Luciferase Reporter (DLR) Assay Systems with the Promega GloMax 20/20 Luminometry System (Promega). Fifty embryos at the blastula stage were collected in 22 µl 1× lysis buffer and vortexed for 1 min. Embryonic lysates were either stored at -80°C or processed immediately. Prior to luciferase readings, 100 µl of the Luciferase Activating Reagent II (LAR-II) was added to each well of the 96-well plate. Then, 20 µl of the embryonic lysates was added and luciferase reading for the firefly was obtained. Subsequently, 100 µl of the Stop and Glow solution was added to quench firefly luciferase (FF) signal and the *Renilla* luciferase (Rluc) reading was obtained. *Renilla* luciferase readings were subtracted from the corresponding initial reading to obtain a firefly reading, which was used to calculate the RLuc/FF ratio. The values of RLuc-containing mutated seed sites were normalized to the corresponding RLuc-containing wild-type miRNA target sites.

Real time, quantitative PCR (QPCR)

One-hundred *Dvl* miRNATP or control TP-injected blastulae were collected. Total RNA was extracted using the Macherey-Nagel Nucleospin RNA Clean-up XS kit according to the manufacturer's instructions. cDNA was synthesized using the iScript cDNA synthesis kit (Bio-Rad). QPCR was performed using 2.5 or 7.5 embryo equivalent for each reaction with the Fast SYBER or PowerUp Green PCR Master Mix

(Thermo Fisher Scientific) in the QuantStudio 6 Real-Time PCR cycler system (Thermo Fisher Scientific). Results were normalized to the mRNA expression of the housekeeping gene *ubiquitin* and shown as fold changes compared with control embryos that were injected with the control morpholino using the $\Delta\Delta C_t$ method as previously described (Stepicheva et al., 2015). Primer sequences were designed using the Primer 3 Program (Rozen and Skaletsky, 2000) and are listed in Table S1. Three to six biological replicates were conducted. Statistical significance was calculated using two-tailed unpaired Student's *t*-tests.

Detection of endogenous AP activity

Activity of endogenous AP was used to assay for differentiated endoderm of the larvae as previously described (Hinman and Degnan, 1998; Drawbridge, 2003; Annunziata et al., 2013; Stepicheva et al., 2015). Because we observed a significant difference in the width of the midgut of control TP- and *Dvl* miRNATP-injected embryos, we used this assay to examine the differentiated endoderm. Five-day-old larvae were fixed in MOPS-paraformaldehyde based fixative (4% paraformaldehyde, 100 mM MOPS pH 7.0, 2 mM $MgSO_4$, 1 mM EGTA and 0.8 M NaCl) for 10 min at room temperature. Embryos were washed with alkaline phosphatase buffer three times (100 mM Tris pH 9.5, 100 mM NaCl, 50 mM $MgCl_2$, 0.1% Tween-20), followed by treatment with the staining solution (0.1 M Tris pH 9.5, 50 mM $MgCl_2$, 0.1 M NaCl, 1 mM levamisole, 10% dimethylformamide, 45 μ l of 75 mg/ml NBT and 35 μ l of 50 mg/ml BCIP per 10 ml of solution). Once the color development was observed, the staining was terminated with washes with MOPS buffer (0.1 M MOPS pH 7.0, 0.5 M NaCl, 0.1% Tween-20). Images were acquired with a Nikon D90 digital camera connected to a Zeiss Observer Z1 microscope.

Immunofluorescence

Gastrula (48 hpf) and larval-stage (120 hpf) embryos were fixed in 4% paraformaldehyde (20% stock; EMS) in artificial sea water overnight at 4°C. Four 10 min PBS-Tween (0.05% Tween-20 in PBS) washes were performed, followed by 1 h of blocking with 4% sheep serum (Sigma-Aldrich). Primary antibody incubation was performed with Endo1 or ID5 antibodies (McClay et al., 1983) at 1:50 overnight at 4°C. Embryos were washed three times for 15 min each with PBS-Tween followed by goat anti-mouse Alexa 488-conjugated secondary antibody (A11001, Thermo Fisher Scientific) at 1:300. After three more PBS-Tween washes, embryos were incubated with Hoechst dye at 1:1000 for 5 min, followed by two more PBS-Tween washes.

To examine the level of *Dvl* protein changes in *Dvl* miRNATP-injected embryos, we injected the control TP and the *Dvl* miRNATP with Texas Red dextran. These 32-cell stage embryos (4–5 hpf) were fixed in 4% paraformaldehyde (20% stock; EMS) in PBS for 20 min, post-fixed with 100% ice cold methanol for 10 min, and washed with several washes of 1× PBS (Peng and Wikramanayake, 2013). Injected embryos were then incubated with primary rabbit anti-SUDDsh-C antibody (Peng and Wikramanayake, 2013; 1:400 overnight at 4°C). Following this incubation, the embryos were washed with PBS-Tween with 0.01% bovine serum albumin three times and then incubated with goat anti-rabbit Alexa 488-conjugated secondary antibody (A11034, Thermo Fisher Scientific) at 1:300. After three more PBS-Tween washes, embryos were incubated with Hoechst dye at 1:1000 for 2 min, followed by three more PBS-Tween washes.

Larval-stage (120 hpf) embryos were fixed in 4% paraformaldehyde (20% stock; EMS) in artificial sea water overnight at 4°C. Four 10 min PBS-Tween washes were performed, followed by 1 h of blocking with 4% sheep serum (Sigma-Aldrich). Double immunofluorescence was performed with primary antibodies overnight at 4°C, using the following dilutions: anti-SUDDsh-C antibody at 1:400 and β -tubulin (Developmental Studies Hybridoma Bank, E7) at 1:10,000. Embryos were washed three times for 15 min each with PBS-Tween followed by 1 h room temperature incubation with goat anti-mouse Alexa 647-conjugated secondary antibody (A-21237, Thermo Fisher Scientific), followed by goat anti-rabbit Cy3 at 1:300, sequentially. After three more PBS-Tween washes, embryos were incubated with Hoechst dye at 1:1000 for 2 min, followed by two more PBS-Tween washes. These immunolabeled embryos in PBS-Tween were mounted onto protamine sulfate-coated slides and imaged using an LSM 780 scanning

confocal microscope (Zeiss Incorporation) and data analysis was performed using Zen software (Zeiss Incorporation).

Dvl protein quantification

To measure semi-quantitatively the amount of *Dvl* in control TP- and *Dvl* miRNATP-treated embryos, confocal z-stack images of 32-cell embryos were collected. The maximum projections of z-stacks of each embryo were collected. The amount of fluorescence pixels were quantified with Metamorph (Molecular Devices). The level of *Dvl* in *Dvl* miRNATP-injected embryos was normalized to that of the control TP-injected embryos.

Phenotyping

To measure DVC length, we took a z-stack of differential interference contrast (DIC) and 1D5-immunolabeled images with a Zeiss Observer Z1 microscope. Normal PMC phenotypes have the following features: (1) sub-equatorial ring formation of PMCs at the vegetal pole of the embryo, (2) anterior migration of the PMCs, and (3) syncytial cables formed among the PMCs. Normal gut phenotypes fulfill the following criteria: (1) fully extended gut tube at gastrula stage and (2) Endo1 antibody staining in mid- and hindgut epithelia. To detect ciliary defects in live embryos, we acquired images using the time-lapse function of an LSM 780 scanning confocal microscope (Zeiss Incorporation).

Statistical analysis

For spicule length, gut/blastopore widths, and expression domains, Student's *t*-tests were used to assess the statistical significance between control and experimental groups. For patterning of PMCs, the Cochran–Mantel–Haenszel test was used to assess the statistical significance of the percentage of normal embryos in the control TP-injected group compared with the *Dvl* miRNATP-injected group. In all graphs, error bars represent s.e.m.

Acknowledgements

We thank Dr David McClay (Duke University) for the 1D5 antibody; Dr Gary Wessel (Brown University) for the Endo1 antibody; Dr Charles Shuster (New Mexico State University) for the mCherry-LifeAct construct; and Dr Deni Galileo (University of Delaware) for the Metamorph program. We also thank the three anonymous reviewers for their valuable feedback.

Competing interests

The authors declare no competing or financial interests.

Author contributions

Conceptualization: J.L.S.; Methodology: N.F.S., N.A.S., J.L.S.; Validation: N.F.S., J.L.S.; Formal analysis: N.F.S., N.A.S., J.L.S.; Investigation: N.F.S., N.A.S., S.A.M.Z., L.W., W.W., J.L.S.; Resources: A.W., J.L.S.; Data curation: N.F.S.; Writing - original draft: N.F.S., J.L.S.; Writing - review & editing: A.W., J.L.S.; Supervision: J.L.S.; Project administration: J.L.S.; Funding acquisition: A.W., J.L.S.

Funding

This work is funded by a National Institutes of Health National Institute of General Medical Sciences grant (5P20GM103653-02-Delaware INBRE), a National Science Foundation CAREER award (IOS 1553338 to J.L.S.) and a National Science Foundation grant (IOS 0754323 to A.W.). Deposited in PMC for release after 12 months.

Supplementary information

Supplementary information available online at <http://dev.biologists.org/lookup/doi/10.1242/dev.167130.supplemental>

References

- Adler, P. N. (2002). Planar signaling and morphogenesis in *Drosophila*. *Dev. Cell* **2**, 525–535.
- Adomako-Ankomah, A. and Ettensohn, C. A. (2013). Growth factor-mediated mesodermal cell guidance and skeletogenesis during sea urchin gastrulation. *Development* **140**, 4214–4225.
- Albertinazzi, C., Cattelino, A. and de Curtis, I. (1999). Rac GTPases localize at sites of actin reorganization during dynamic remodeling of the cytoskeleton of normal embryonic fibroblasts. *J. Cell Sci.* **112**, 3821–3831.
- Annunziata, R., Perillo, M., Andrikou, C., Cole, A. G., Martinez, P. and Arnone, M. I. (2013). Pattern and process during sea urchin gut morphogenesis: the regulatory landscape. *Genesis* **52**, 251–268.

- Axelrod, J. D., Miller, J. R., Shulman, J. M., Moon, R. T. and Perrimon, N. (1998). Differential recruitment of Dishevelled provides signaling specificity in the planar cell polarity and Wingless signaling pathways. *Genes Dev.* **12**, 2610-2622.
- Bartel, D. P. (2009). MicroRNAs: target recognition and regulatory functions. *Cell* **136**, 215-233.
- Burke, R. D. (1981). Structure of the digestive tract of the pluteus larva of *Dendraster excentricus* (Echinodermata: Echinoida). *Zoomorphology* **98**, 209-225.
- Burke, R. D. and Alvarez, C. M. (1988). Development of the esophageal muscles in embryos of the sea urchin *Strongylocentrotus purpuratus*. *Cell Tissue Res.* **252**, 411-417.
- Burke, R. D., Moller, D. J., Krupke, O. A. and Taylor, V. J. (2014). Sea urchin neural development and the metazoan paradigm of neurogenesis. *Genesis* **52**, 208-221.
- Byrum, C. A., Xu, R., Bince, J. M., McClay, D. R. and Wikramanayake, A. H. (2009). Blocking Dishevelled signaling in the noncanonical Wnt pathway in sea urchins disrupts endoderm formation and spiculogenesis, but not secondary mesoderm formation. *Dev. Dyn.* **238**, 1649-1665.
- Caron, A., Xu, X. and Lin, X. (2012). Wnt/beta-catenin signaling directly regulates Foxj1 expression and ciliogenesis in zebrafish Kupffer's vesicle. *Development* **139**, 514-524.
- Cheers, M. S. and Ettensohn, C. A. (2004). Rapid microinjection of fertilized eggs. *Methods Cell Biol.* **74**, 287-310.
- Chung, C. Y., Lee, S., Briscoe, C., Ellsworth, C. and Firtel, R. A. (2000). Role of Rac in controlling the actin cytoskeleton and chemotaxis in motile cells. *Proc. Natl. Acad. Sci. USA* **97**, 5225-5230.
- Crain, W. R., Jr. and Bushman, F. D. (1983). Transcripts of paternal and maternal actin gene alleles are present in interspecific sea urchin embryo hybrids. *Dev. Biol.* **100**, 190-196.
- Cui, M., Siriwon, N., Li, E., Davidson, E. H. and Peter, I. S. (2014). Specific functions of the Wnt signaling system in gene regulatory networks throughout the early sea urchin embryo. *Proc. Natl. Acad. Sci. USA* **111**, E5029-E5038.
- Dale, R. M., Sisson, B. E. and Topczewski, J. (2009). The emerging role of Wnt/PCP signaling in organ formation. *Zebrafish* **6**, 9-14.
- Darken, R. S., Scola, A. M., Rakeman, A. S., Das, G., Mlodzik, M. and Wilson, P. A. (2002). The planar polarity gene strabismus regulates convergent extension movements in *Xenopus*. *EMBO J.* **21**, 976-985.
- De, A. (2011). Wnt/Ca²⁺ signaling pathway: a brief overview. *Acta Biochim. Biophys. Sin.* **43**, 745-756.
- Drawbridge, J. (2003). The color purple: analyzing alkaline phosphatase expression in experimentally manipulated sea urchin embryos in an undergraduate developmental biology course. *Int. J. Dev. Biol.* **47**, 161-164.
- Duboc, V., Lapraz, F., Saudemont, A., Bessodes, N., Mekpoh, F., Hailot, E., Quirin, M. and Lepage, T. (2010). Nodal and BMP2/4 pattern the mesoderm and endoderm during development of the sea urchin embryo. *Development* **137**, 223-235.
- Duloquin, L., Lhomond, G. and Gache, C. (2007). Localized VEGF signaling from ectoderm to mesenchyme cells controls morphogenesis of the sea urchin embryo skeleton. *Development* **134**, 2293-2302.
- Ettensohn, C. A. and Dey, D. (2017). Kirrell, a member of the Ig-domain superfamily of adhesion proteins, is essential for fusion of primary mesenchyme cells in the sea urchin embryo. *Dev. Biol.* **421**, 258-270.
- Ettensohn, C. A., Illies, M. R., Oliveri, P. and De Jong, D. L. (2003). Alx1, a member of the Cart1/Alx3/Alx4 subfamily of Paired-class homeodomain proteins, is an essential component of the gene network controlling skeletogenic fate specification in the sea urchin embryo. *Development* **130**, 2917-2928.
- Ettensohn, C. A., Wessel, G. M. and Wray, G. A. (2004). Methods in cell biology. In *Development of Sea Urchins, Ascidians, and other Invertebrate Deuterostomes: Experimental Approaches* (ed. C. A. Ettensohn, G. M. Wessel and G. A. Wray), pp. 1-13. San Diego: Elsevier Academic Press.
- Ewald, A. J., Peyrot, S. M., Tyska, J. M., Fraser, S. E. and Wallingford, J. B. (2004). Regional requirements for Dishevelled signaling during *Xenopus* gastrulation: separable effects on blastopore closure, mesendoderm internalization and archenteron formation. *Development* **131**, 6195-6209.
- Gao, C. and Chen, Y.-G. (2010). Dishevelled: the hub of Wnt signaling. *Cell. Signal.* **22**, 717-727.
- Gregory, P. A., Bert, A. G., Paterson, E. L., Barry, S. C., Tsykin, A., Farshid, G., Vadas, M. A., Khew-Goodall, Y. and Goodall, G. J. (2008). The miR-200 family and miR-205 regulate epithelial to mesenchymal transition by targeting ZEB1 and SIP1. *Nat. Cell Biol.* **10**, 593-601.
- Gubb, D. and Garcia-Bellido, A. (1982). A genetic analysis of the determination of cuticular polarity during development in *Drosophila melanogaster*. *J. Embryol. Exp. Morphol.* **68**, 37-57.
- Hayes, M., Naito, M., Daulat, A., Angers, S. and Ciruna, B. (2013). Ptk7 promotes non-canonical Wnt/PCP-mediated morphogenesis and inhibits Wnt/beta-catenin-dependent cell fate decisions during vertebrate development. *Development* **140**, 1807-1818.
- He, H., Chen, K., Wang, F., Zhao, L., Wan, X., Wang, L. and Mo, Z. (2015). miR-204-5p promotes the adipogenic differentiation of human adipose-derived mesenchymal stem cells by modulating DVL3 expression and suppressing Wnt/beta-catenin signaling. *Int. J. Mol. Med.* **35**, 1587-1595.
- Hinman, V. F. and Degnan, B. M. (1998). Retinoic acid disrupts anterior ectodermal and endodermal development in ascidian larvae and postlarvae. *Dev. Genes Evol.* **208**, 336-345.
- Howard, E. W., Newman, L. A., Oleksyn, D. W., Angerer, R. C. and Angerer, L. M. (2001). SpKrl: a direct target of beta-catenin regulation required for endoderm differentiation in sea urchin embryos. *Development* **128**, 365-375.
- Huang, X., Wang, Z., Li, D., Huang, Z., Dong, X., Li, C. and Lan, J. (2018). Study of microRNAs targeted Dvl2 on the osteoblasts differentiation of rat BMSCs in hyperlipidemia environment. *J. Cell. Physiol.* **233**, 6758-6766.
- Kang, S.-H., Cho, M.-J. and Kole, R. (1998). Up-regulation of luciferase gene expression with antisense oligonucleotides: implications and applications in functional assay development. *Biochemistry* **37**, 6235-6239.
- Kinukawa, M. and Vacquier, V. D. (2007). Recombinant sea urchin flagellar adenylate kinase. *J. Biochem.* **142**, 501-506.
- Komiyama, Y. and Habas, R. (2008). Wnt signal transduction pathways. *Organogenesis* **4**, 68-75.
- Kühl, M., Sheldahl, L. C., Malbon, C. C. and Moon, R. T. (2000). Ca(2+)/calmodulin-dependent protein kinase II is stimulated by Wnt and Frizzled homologs and promotes ventral cell fates in *Xenopus*. *J. Biol. Chem.* **275**, 12701-12711.
- Kumano, G. and Nishida, H. (1998). Maternal and zygotic expression of the endoderm-specific alkaline phosphatase gene in embryos of the ascidian, *Halocynthia roretzi*. *Dev. Biol.* **198**, 245-252.
- Kumburegama, S., Wijesena, N., Xu, R. and Wikramanayake, A. H. (2011). Strabismus-mediated primary archenteron invagination is uncoupled from Wnt/beta-catenin-dependent endoderm cell fate specification in *Nematostella vectensis* (Anthozoa, Cnidaria): Implications for the evolution of gastrulation. *Evodevo* **2**, 2.
- Kunimoto, K., Yamazaki, Y., Nishida, T., Shinohara, K., Ishikawa, H., Hasegawa, T., Okanoue, T., Hamada, H., Noda, T., Tamura, A. et al. (2012). Coordinated ciliary beating requires Odf2-mediated polarization of basal bodies via basal feet. *Cell* **148**, 189-200.
- Lee, P. N., Kumburegama, S., Marlow, H. Q., Martindale, M. Q. and Wikramanayake, A. H. (2007). Asymmetric developmental potential along the animal-vegetal axis in the anthozoan cnidarian, *Nematostella vectensis*, is mediated by Dishevelled. *Dev. Biol.* **310**, 169-186.
- Lin, X. and Xu, X. (2009). Distinct functions of Wnt/beta-catenin signaling in KV development and cardiac asymmetry. *Development* **136**, 207-217.
- Lindqvist, M., Horn, Z., Bryja, V., Schulte, G., Papachristou, P., Ajima, R., Dyberg, C., Arenas, E., Yamaguchi, T. P., Lagercrantz, H. et al. (2010). Vang-like protein 2 and Rac1 interact to regulate adherens junctions. *J. Cell Sci.* **123**, 472-483.
- Logan, C. Y., Miller, J. R., Ferkowicz, M. J. and McClay, D. R. (1999). Nuclear beta-catenin is required to specify vegetal cell fates in the sea urchin embryo. *Development* **126**, 345-357.
- Marshall, W. F. and Kintner, C. (2008). Cilia orientation and the fluid mechanics of development. *Curr. Opin. Cell Biol.* **20**, 48-52.
- McClay, D. R., Cannon, G. W., Wessel, G. M., Fink, R. D. and Marchase, R. B. (1983). Patterns of antigenic expression in early sea urchin development. In *Time, Space, and Pattern in Embryonic Development* (ed. W. R. J. a. R. A. Raff), pp. 157-169. New York: A.R. Liss.
- McIntyre, D. C., Seay, N. W., Croce, J. C. and McClay, D. R. (2013). Short-range Wnt5 signaling initiates specification of sea urchin posterior ectoderm. *Development* **140**, 4881-4889.
- Minegishi, K., Hashimoto, M., Ajima, R., Takaoka, K., Shinohara, K., Ikawa, Y., Nishimura, H., McMahon, A. P., Willert, K., Okada, Y. et al. (2017). A Wnt5 activity asymmetry and intercellular signaling via PCP proteins polarize node cells for left-right symmetry breaking. *Dev. Cell* **40**, 439-452.e4.
- Mito, T., Okamoto, H., Shinahara, W., Shinmyo, Y., Miyawaki, K., Ohuchi, H. and Noji, S. (2006). Kruppel acts as a gap gene regulating expression of hunchback and even-skipped in the intermediate germ cricket *Gryllus bimaculatus*. *Dev. Biol.* **294**, 471-481.
- Mizuno, K., Shiba, K., Yaguchi, J., Shibata, D., Yaguchi, S., Prulière, G., Chenevert, J. and Inaba, K. (2017). Calaxin establishes basal body orientation and coordinates movement of monocilia in sea urchin embryos. *Sci. Rep.* **7**, 10751.
- Mlodzik, M. (2016). The dishevelled protein family: still rather a mystery after over 20 years of molecular studies. *Curr. Top. Dev. Biol.* **117**, 75-91.
- Momose, T., Kraus, Y. and Houlston, E. (2012). A conserved function for Strabismus in establishing planar cell polarity in the ciliated ectoderm during cnidarian larval development. *Development* **139**, 4374-4382.
- Moon, R. T. (2005). Wnt/beta-catenin pathway. *Sci. STKE* **2005**, cm1.
- Nicolas, F. E. (2011). Experimental validation of microRNA targets using a luciferase reporter system. *Methods Mol. Biol.* **732**, 139-152.
- Otim, O. (2017). An empirical model of Onecut binding activity at the sea urchin SM50 C-element gene regulatory region. *Int. J. Dev. Biol.* **61**, 537-543.
- Otim, O., Amore, G., Minokawa, T., McClay, D. R. and Davidson, E. H. (2004). SpHnf6, a transcription factor that executes multiple functions in sea urchin embryogenesis. *Dev. Biol.* **273**, 226-243.

- Park, T. J., Mitchell, B. J., Abitua, P. B., Kintner, C. and Wallingford, J. B. (2008). Dishevelled controls apical docking and planar polarization of basal bodies in ciliated epithelial cells. *Nat. Genet.* **40**, 871-879.
- Peng, C. F. and Wikramanayake, A. H. (2013). Differential regulation of Dishevelled in a novel vegetal cortical domain in sea urchin eggs and embryos: Implications for the localized activation of canonical Wnt signaling. *PLoS ONE* (in press) **8**, e80693.
- Peter, I. S. and Davidson, E. H. (2010). The endoderm gene regulatory network in sea urchin embryos up to mid-blastula stage. *Dev. Biol.* **340**, 188-199.
- Peter, I. S. and Davidson, E. H. (2011). A gene regulatory network controlling the embryonic specification of endoderm. *Nature* **474**, 635-639.
- Piacentino, M. L., Ramachandran, J. and Bradham, C. A. (2015). Late Alk4/5/7 signaling is required for anterior skeletal patterning in sea urchin embryos. *Development* **142**, 943-952.
- Piacentino, M. L., Zuch, D. T., Fishman, J., Rose, S., Speranza, E. E., Li, C., Yu, J., Chung, O., Ramachandran, J., Ferrell, P. et al. (2016). RNA-Seq identifies SPGs as a ventral skeletal patterning cue in sea urchins. *Development* **143**, 703-714.
- Range, R. C., Angerer, R. C. and Angerer, L. M. (2013). Integration of canonical and noncanonical Wnt signaling pathways patterns the neuroectoderm along the anterior-posterior axis of sea urchin embryos. *PLoS Biol.* **11**, e1001467.
- Riedl, J., Crevenna, A. H., Kessenbrock, K., Yu, J. H., Neukirchen, D., Bista, M., Bradke, F., Jenne, D., Holak, T. A., Werb, Z. et al. (2008). Lifeact: a versatile marker to visualize F-actin. *Nat. Methods* **5**, 605-607.
- Rottinger, E., Saudemont, A., Duboc, V., Besnardeau, L., McClay, D. and Lepage, T. (2008). FGF signals guide migration of mesenchymal cells, control skeletal morphogenesis [corrected] and regulate gastrulation during sea urchin development. *Development* **135**, 353-365.
- Rozen, S. and Skaletsky, H. (2000). Primer3 on the WWW for general users and for biologist programmers. *Methods Mol. Biol.* **132**, 365-386.
- Schueler, M., Braun, D. A., Chandrasekar, G., Gee, H. Y., Klasson, T. D., Halbritter, J., Bieder, A., Porath, J. D., Airik, R., Zhou, W. et al. (2015). DCC2 mutations cause a renal-hepatic ciliopathy by disrupting Wnt signaling. *Am. J. Hum. Genet.* **96**, 81-92.
- Selbach, M., Schwanhäusser, B., Thierfelder, N., Fang, Z., Khanin, R. and Rajewsky, N. (2008). Widespread changes in protein synthesis induced by microRNAs. *Nature* **455**, 58-63.
- Sepich, D. S., Usmani, M., Pawlicki, S. and Solnica-Krezel, L. (2011). Wnt/PCP signaling controls intracellular position of MTOCs during gastrulation convergence and extension movements. *Development* **138**, 543-552.
- Simons, M. and Mlodzik, M. (2008). Planar cell polarity signaling: from fly development to human disease. *Annu. Rev. Genet.* **42**, 517-540.
- Sokol, S. Y. (1996). Analysis of Dishevelled signalling pathways during Xenopus development. *Curr. Biol.* **6**, 1456-1467.
- Song, J. L., Stoeckius, M., Maaskola, J., Friedländer, M., Stepicheva, N., Juliano, C., Lebedeva, S., Thompson, W., Rajewsky, N. and Wessel, G. M. (2012). Select microRNAs are essential for early development in the sea urchin. *Dev. Biol.* **362**, 104-113.
- Song, J. L., Nigam, P., Tektas, S. S. and Selva, E. (2015). microRNA regulation of Wnt signaling pathways in development and disease. *Cell. Signal.* **27**, 1380-1391.
- Staton, A. A. and Giraldez, A. J. (2011). Use of target protector morpholinos to analyze the physiological roles of specific miRNA-mRNA pairs in vivo. *Nat. Protoc.* **6**, 2035-2049.
- Stepicheva, N. A. and Song, J. L. (2014). High throughput microinjections of sea urchin zygotes. *J. Vis. Exp.* e50841.
- Stepicheva, N. A. and Song, J. L. (2015). microRNA-31 modulates skeletal patterning in the sea urchin embryos. *Development* **142**, 3769-3780.
- Stepicheva, N., Nigam, P. A., Siddam, A. D., Peng, C. F. and Song, J. L. (2015). microRNAs regulate beta-catenin of the Wnt signaling pathway in early sea urchin development. *Dev. Biol.* **402**, 127-141.
- Stepicheva, N. A., Dumas, M., Kobi, P., Donaldson, J. G. and Song, J. L. (2017). The small GTPase Arf6 regulates sea urchin morphogenesis. *Differentiation* **95**, 31-43.
- Sun, Z. and Ettensohn, C. A. (2017). TGF-beta sensu stricto signaling regulates skeletal morphogenesis in the sea urchin embryo. *Dev. Biol.* **421**, 149-160.
- Tada, M. and Smith, J. C. (2000). Xwnt11 is a target of Xenopus Brachyury: regulation of gastrulation movements via Dishevelled, but not through the canonical Wnt pathway. *Development* **127**, 2227-2238.
- Tauriello, D. V. F., Jordens, I., Kirchner, K., Slootstra, J. W., Kruitwagen, T., Bouwman, B. A. M., Noutsou, M., Rudiger, S. G. D., Schwamborn, K., Schambony, A. et al. (2012). Wnt/beta-catenin signaling requires interaction of the Dishevelled DEP domain and C terminus with a discontinuous motif in Frizzled. *Proc. Natl. Acad. Sci. USA* **109**, E812-E820.
- Weitzel, H. E., Illies, M. R., Byrum, C. A., Xu, R., Wikramanayake, A. H. and Ettensohn, C. A. (2004). Differential stability of beta-catenin along the animal-vegetal axis of the sea urchin embryo mediated by dishevelled. *Development* **131**, 2947-2956.
- Wessel, G. M. and McClay, D. R. (1985). Sequential expression of germ-layer specific molecules in the sea urchin embryo. *Dev. Biol.* **111**, 451-463.
- Whittaker, J. R. (1990). Determination of alkaline phosphatase expression in endodermal cell lineages of an ascidian embryo. *Biol. Bulletin* **178**, 222-230.
- Yaguchi, S., Yaguchi, J., Angerer, R. C. and Angerer, L. M. (2008). A Wnt-FoxQ2-nodal pathway links primary and secondary axis specification in sea urchin embryos. *Dev. Cell* **14**, 97-107.
- Yaguchi, S., Yaguchi, J., Angerer, R. C., Angerer, L. M. and Burke, R. D. (2010). TGFbeta signaling positions the ciliary band and patterns neurons in the sea urchin embryo. *Dev. Biol.* **347**, 71-81.
- Yamazaki, A., Kawabata, R., Shiomi, K., Tsuchimoto, J., Kiyomoto, M., Amemiya, S. and Yamaguchi, M. (2008). Kruppel-like is required for nonskeletogenic mesoderm specification in the sea urchin embryo. *Dev. Biol.* **314**, 433-442.
- Yin, C., Ciruna, B. and Solnica-Krezel, L. (2009). Convergence and extension movements during vertebrate gastrulation. *Curr. Top. Dev. Biol.* **89**, 163-192.
- Yoshida, Y., Kim, S., Chiba, K., Kawai, S., Tachikawa, H. and Takahashi, N. (2004). Calcineurin inhibitors block dorsal-side signaling that affect late-stage development of the heart, kidney, liver, gut and somitic tissue during Xenopus embryogenesis. *Dev. Growth Differ.* **46**, 139-152.
- Zhang, Y., Ding, Y., Chen, Y.-G. and Tao, Q. (2014). NEDD4L regulates convergent extension movements in Xenopus embryos via Dishevelled-mediated non-canonical Wnt signaling. *Dev. Biol.* **392**, 15-25.
- Zhu, P., Xu, X. and Lin, X. (2015). Both ciliary and non-ciliary functions of Foxj1a confer Wnt/beta-catenin signaling in zebrafish left-right patterning. *Biol. Open* **4**, 1376-1386.